Contents lists available at ScienceDirect

Science of the Total Environment

journal homepage: www.elsevier.com/locate/scitotenv

Hydroclimatic relationships and stable isotopic analysis in baldcypress tree rings

Jared M. Friedman [a,1], Emily A. Elliott [a,b,*], Clay S. Tucker [c,**], Joshua C. Bregy [d], Matthew D. Therrell [a], Jessie K. Pearl [e]

[a] Department of Geography and the Environment, The University of Alabama, Box 870322, Tuscaloosa, AL 35401, United States of America
[b] New College, The University of Alabama, Box 870229, Tuscaloosa, AL 35401, United States of America
[c] School of Biological, Environmental and Earth Sciences, The University of Southern Mississippi, 103 Bobby Chain Technology Center, 118 College Dr. #5018, Hattiesburg, MS 39406, United States of America
[d] Department of Environmental Engineering and Earth Sciences, 445 Bracket Hall, Clemson, SC 29634, United States of America
[e] The Nature Conservancy, 1510 E. Fort Lowell Road, Tucson, AZ 85719, United States of America

HIGHLIGHTS

- Tree-ring stable oxygen isotopes for drought, streamflow, and tropical cyclone reconstruction
- Interspecies comparison of baldcypress with longleaf pine
- Strong indication of hydroclimatic extremes

GRAPHICAL ABSTRACT

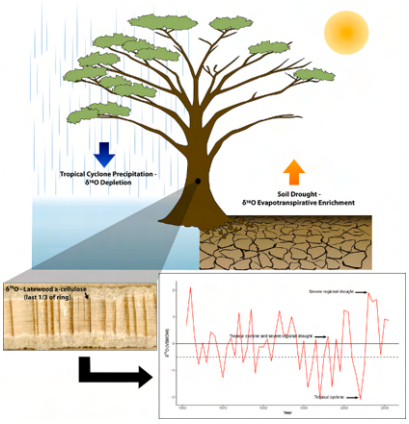

ABSTRACT

Instrumental records of hydroclimatic extremes (e.g., drought, pluvial flooding, tropical cyclones) are temporally and spatially limited, making long-term assessments of the drivers of these events difficult. Paleo-reconstructions of these extreme events are therefore essential in understanding and evaluating future risk, especially within vulnerable coastal communities. In dendrochronology, $\delta^{18}O$ ($^{18}O/^{16}O$) is a known proxy for reconstructing various hydroclimatic parameters (i.e., temperature, atmospheric humidity, streamflow). The tree takes up $\delta^{18}O$ in source water for the development of woody tissue, with the isotopic ratio stored within the α-cellulose of annual tree rings. However, cellulose-derived $\delta^{18}O$ from baldcypress (*Taxodium distichum*), the longest-lived species in the region, has never been investigated in studies of hydroclimate. In this exploratory study, we evaluate the use of $\delta^{18}O$-depletion in baldcypress latewood as a proxy for various southeastern hydroclimatic extremes to the comparable instrumental period. Results of baldcypress latewood $\delta^{18}O$ over the Choctawhatchee River Basin were then compared to

* Correspondence to: E.A. Elliott, Department of Geography and the Environment, The University of Alabama, Box 870322, Tuscaloosa, AL 35401, United States of America
** Corresponding author.
E-mail addresses: emily.elliott@ua.edu (E.A. Elliott), clay.tucker@usm.edu (C.S. Tucker).
[1] Present address: Agriculture Building, Room 119, 1000 E. University Ave., Laramie, WY 82071.

https://doi.org/10.1016/j.scitotenv.2025.180392
Received 15 January 2025; Received in revised form 12 August 2025; Accepted 29 August 2025
Available)online)19)September)2025)

various climate indices and the instrumental tropical cyclone record, with correlations of varying strength expressed between the produced $\delta^{18}O$ time series and precipitation, streamflow, self-calibrated Palmer Drought Severity Index, and maximum summer temperature. Large decreases in baldcypress $\delta^{18}O$ latewood are determined to be reflective of regional TC precipitation. In direct interspecies comparisons, baldcypress $\delta^{18}O$ is shown to be more sensitive to drought conditions than nearby longleaf pine (*Pinus palustris*) $\delta^{18}O$. Results of these comparisons reveal the future potential of the proxy in multivariate climate reconstructions.

1. Introduction

1.1. Background

The northern Gulf Coast (GC) historically experiences intense hydroclimatic extremes, including droughts, pluvials and tropical cyclone (TC) activity, the latter of which can occur as often as every other year (Knutson and Tuleya, 2004; Keim et al., 2007; Paerl et al., 2019; Sadeghi et al., 2019a; Knutson et al., 2020). The GC also experiences high rates of coastal subsidence (~4.5–8 mm/yr; Kolker et al., 2011) and associated relative sea-level rise (~10 mm/yr; Desantis et al., 2007). The flat, low-lying coastal plains along the GC leave communities at disproportionate risk of damage from heavy precipitation, strong winds and storm surge (Gornitz et al., 1994). Despite this vulnerability, the GC ranks as the fastest-growing coastal region in the US (U.S. Census Bureau, 2019). This highlights the urgency to better understand the hydroclimatic extremes in the southeastern U.S. and the role anthropogenic climate change plays in future hydroclimatic shifts in the GC. Determining whether the effects of anthropogenic forcing exceed natural variability is challenging in this region due to the limited instrumental and historical data (Neumann, 1987; Therrell et al., 2020; Tucker et al., 2022). Long-term records of hydroclimatic shifts are critical to contextualizing climate projections and need further development throughout the region (Williams et al., 2020; Williams et al., 2022). To extend the record of TC activity both spatially and temporally, paleo-proxy data are used to reconstruct long-term, high-resolution records documenting changes in hydroclimatic variability over time (Mann et al., 2007; Mann et al., 2009; Wallace et al., 2019; Oliva et al., 2018). Specifically, tree-ring proxies are used to record climate variability, reconstruct hydroclimatic extremes, and record TC frequency at annual resolution over multiple centuries (Miller et al., 2006; Knapp et al., 2016; Copenheaver et al., 2017; Therrell et al., 2020; Knapp et al., 2021; Maxwell et al., 2021; Bregy et al., 2022; Tucker et al., 2022). Regional paleo-reconstructions of water availability in western U.S. forests are common (Cook et al., 1999; Stahle et al., 2003; Cook et al., 2004; Woodhouse et al., 2006; Woodhouse et al., 2010; Williams et al., 2013; Cook et al., 2015; King et al., 2024a). However, paleo-drought in the southeastern United States has been given comparatively less attention, resulting in a less comprehensive understanding of hydroclimatic variability in the region. With recently observed water shortages, over-allocation of rapidly depleting groundwater resources in metropolitan areas, and high agricultural drought variability, developing a better understanding of water resource availability in the region is imperative (Manuel, 2008; Pederson et al., 2012; Kuwayama et al., 2019; Sadeghi et al., 2019b). More recently, efforts to reconstruct streamflow, precipitation and temperature using dendrochronological archives have facilitated a better understanding of the long-term climate drivers of droughts and pluvial events throughout the southeastern U.S. (Stahle et al., 1985a, 1985b; Stahle and Cleaveland, 1992; Stahle et al., 1998; Therrell and Bialecki, 2015; Anderson et al., 2019; Therrell et al., 2020; King et al., 2024b). While tree-ring records are typically representative of a single river or watershed, pairing records from across the region allows for increased spatiotemporal resolution of hydroclimatic analysis (Vines et al., 2021; King et al., 2024a, 2024b).

1.2. False rings

In addition to tree-ring width, analysis of anatomical anomalies in tree rings is common for disturbance reconstruction (Schweingruber, 1993; Sheppard et al., 2008; Bräuning et al., 2016; Margolis et al., 2022). Similar patterns of intra-annual density fluctuations have been documented in other North American species along the northern Gulf of Mexico, (Knapp et al., 2016; Mitchell et al., 2019; Knapp et al., 2021), and while not a one-to-one proxy, these anatomical approaches to building sub-seasonal records show tremendous potential to extend the highly resolved record of hydroclimatic extremes back in time.

In baldcypress (*Taxodium distichum)*, false rings, or anomalous bands of latewood, can be correlated with TC activity (Copenheaver et al., 2017; Therrell et al., 2020; Tucker et al., 2022). In the southeastern U.S., TCs typically occur in the late summer/ fall, after the point at which baldcypress begins latewood production. The rapid influx of available late summer floodwater spurs a re-starting of earlywood production, leaving a band of latewood sandwiched between two portions of earlywood grown within the same year (Therrell et al., 2020). Years in which a high percentage of false rings were observed between trees without the occurrence of a TC (~23 %) were hypothesized to be the result of anomalously high frontal precipitation (Tucker et al., 2022).

1.3. Oxygen isotopes

Previous research has assessed various baldcypress tree-ring proxies against climate parameters including ring-width indices (Stahle et al., 2012), false-ring chronologies (Therrell et al., 2020), and suppression chronologies (Tucker et al., 2018). Objectives of this study expanded upon previous success with baldcypress dendrochronology to understand the processes involved in stable isotopic composition. Stable isotopic composition of tree-ring samples aims to understand finer-scale environmental drivers of growth beyond traditional ring-width analyses. Stable oxygen isotopic analysis, or the ratio of $^{16}O/^{18}O$ ($\delta^{18}O$), measures fractionation that occurs primarily within source water (Epstein et al., 1977; Lawrence and Gedzelman, 1996). When water that is depleted or enriched in ^{18}O is taken up trees and used in the development of woody tissue, the isotopic ratio is stored within the α-cellulose of latewood in annual growth rings (Sternberg and Deniro, 1983; McCarroll and Loader, 2004; Miller et al., 2006; Gessler et al., 2014; Andreu-Hayles et al., 2022). Studies analyzed cellulose $\delta^{18}O$ for relationships with temperature (e.g., Burk and Stuiver, 1981; Feng and Epstein, 1994; Porter et al., 2014; Szejner et al., 2021), broad-scale climate modes (e.g., Li et al., 2011; Brienen et al., 2012), atmospheric humidity (e.g., Edwards et al., 1985; Roden and Ehleringer, 2000), precipitation (e.g., Dansgaard, 1964; Ramesh et al., 1986; Xu et al., 2021), streamflow (e.g., Barbour et al., 2002; Raffalli-Delerce et al., 2004), and to a very limited extent, TC reconstructions (Miller et al., 2006; Nelson, 2008; Labotka et al., 2016; Li et al., 2011; Lewis et al., 2011; Altman et al., 2021).

The use of tree-ring stable oxygen isotopic analysis has strong potential for reconstructing TC activity. Compared to frontal rain, TC precipitation can be as much as 10–20 ‰ depleted in ^{18}O (Gedzelman and Arnold, 1994). This ^{18}O depletion occurs in spiral rainbands outside the eyewall of the TC, radiating outward as far as 120 km in any given direction (Lawrence, 1998; Lawrence et al., 2002). ^{18}O-depleted precipitation is taken up by trees and stored in the latewood portion of annual growth rings (Epstein et al., 1977; Lawrence and Gedzelman, 1996; Tang and Feng, 2001; McCarroll and Loader, 2004; Miller et al., 2006). The precise intra-ring location is likely impacted by the overlap of species-dependent xylogenesis and the seasonality of regional TCs (Song et al., 2014; Belmecheri et al., 2018). Isotopic anomalies originating in the source water can be recorded and compared to

instrumental and historical TC records. The use of stable isotopic analysis in tree rings to reconstruct TC activity was first validated in Miller et al. (2006), where significant isotopic ^{18}O depletion in nearby longleaf pine (*Pinus palustris)* tree rings was correlated with TC activity occurring within ~400 km of the sample site in Valdosta, GA. That research was later corroborated by Nelson (2008) in the western Florida panhandle at the Eglin Airforce Base and additional work in southern Georgia by Labotka et al. (2016), developing records from longleaf pine cores and subfossil wood to reconstruct over 400 years of TC precipitation. Additional southeastern $\delta^{18}O$ TC records have successfully been developed using longleaf pine and other relatively short-lived species of the genus *Pinus*, including *P. elliottii, P. virginiana*, and *P. strobus* (Miller et al., 2006; Li et al., 2011; Lewis et al., 2011).

1.4. Baldcypress (*Taxodium distichum*)

Baldcypress, a prevalent species throughout the southeastern U.S., has proven to be an excellent species for the development of millennial-length high-resolution hydroclimatic reconstructions. The extremely long-lived species thrives in alluvial floodplains, where surface water collects from throughout the watershed and is taken up by the shallow root system (Stahle et al., 1985a; Stahle et al., 1985b). Baldcypress has been successfully used in dendrochronological studies of southeastern climate/hydroclimate, with much of this research establishing strong relationships between annual or seasonal ring width, and precipitation, streamflow, temperature, and various drought indices (Stahle et al., 1985a; Stahle et al., 1985b; Stahle and Cleaveland, 1992; Stahle and Cleaveland, 1994; Stahle et al., 2012; Therrell et al., 2020). Given baldcypress' distribution and growth characteristics, there is strong potential in applying novel dendrochronological applications to expand the proxy opportunities of the species. To date, no published research has documented the use of this species in the development of climate reconstructions using stable oxygen isotopic analysis.

Although baldcypress is responsible for the most well-resolved climate reconstructions throughout the south and southeastern United States, the relationship between hydroclimatic variables and $\delta^{18}O$ in baldcypress α-cellulose has yet to be explored. Limited use of the species in wetland ecology research has suggested both the primary use of meteoric precipitation as the species' source water and an interpretable isotopic response (Hsueh et al., 2016). The species-specific response to hydroclimatic events is poorly understood, necessitating a preliminary exploration of stable oxygen isotopic analysis as a proxy in baldcypress for the purpose of long-term climate reconstruction. While ring-width records have been largely successful in providing annual and seasonal records of precipitation, streamflow, temperature, and drought, α-cellulose $\delta^{18}O$ is a more direct measure of processes that occur in the source water, largely independent from the tree itself. While the tree undoubtedly influences this relationship, no significant isotopic response has been recorded from intra-tree fractionation when compared to that occurring within the source water (Dawson and Ehleringer, 1991; Dawson, 1993; Song et al., 2014).

Here, we investigate the potential climate drivers of $\delta^{18}O$ variation in baldcypress growth rings and determine whether the proxy can be used to study elements of hydroclimatic variability not captured with ring width alone. The spatiotemporal relationships between these records and various climate variables such as precipitation, streamflow, summer max temperature, and Palmer Drought Severity Index are investigated. Additionally, we investigate the potential of baldcypress $\delta^{18}O$ in extreme-event-based TC analysis. We discuss applications of the proxy and its utility in records of tropical cyclone precipitation, an avenue of active investigation.

2. Materials and methods

2.1. Study area

For this study, we used previously collected tree cores from a site located near Choctawhatchee Bay, FL for $\delta^{18}O$ analysis. The site is made up of coastal bottomland hardwood forests, characterized by low elevation (<50 m above sea level) and a subtropical climate with wet summers and dry winters. These baldcypress, swamp tupelo (*Nyssa biflora*), and ash (*Fraxinus* spp.) dominated forests flood on a regular basis, with poorly-drained entisols and low infiltration rates allowing surface-water to pond throughout the year. Late-summer flooding, most commonly a result of TC precipitation, pools in the delta and interfaces with seawater, leading to the development of coastal swamps. Because of logging culls, sinker logs, and buried subfossil wood, baldcypress swamps are home to some of the last remaining old-growth forests and subfossil wood in the eastern United States (Mattoon, 1915). These characteristics made this site ideal for tree-ring analysis, with baldcypress cores initially collected for use in studies of southeastern hydroclimate (Stahle et al., 2012; Therrell et al., 2020; Vines et al., 2021; Tucker et al., 2022; Fig. 1). Early results published with cores from the same site location identified a strong correlation ($r \simeq 0.71–0.84$) between spring rainfall and total ring width (Stahle and Cleaveland, 1994). Multiple sites were used alongside streamflow gauges to reconstruct ~800 years of regional streamflow variability, identifying patterns of hydroclimatic extremes consistent between five distinct rivers (Vines et al., 2021). Additionally, previous studies have assessed these relationships (including with $\delta^{18}O$) with sites of longleaf pine, including a site from Eglin Airforce Base, FL (hence forth referred to as the Eglin Airforce Base Longleaf Pine record or E-LP-LW) and a site near Valdosta, GA (hence forth referred to as the Valdosta Longleaf Pine Latewood record or V-LP-LW), with promising results (Miller et al., 2006, Nelson, 2008, and Labotka et al., 2016; Fig. 1).

Prior to use in this study, work by Therrell et al. (2020) and Tucker et al. (2022) identified a relationship between tropical cyclones and false ring occurrence, linking a secondary spurt of earlywood growth to the late summer flooding typical of southeastern TCs. Years in which ≥20 % of sampled trees from across the northern Gulf of Mexico contained a false ring were considered “high false-ring years,” 77 % of which were associated with a landfalling tropical cyclone within 223 km of the site. These findings prompted our investigation into the link between baldcypress $\delta^{18}O$ and tropical cyclones, with the goal of determining whether the novel method will yield a comparable relationship between baldcypress source- water and TC precipitation. From the approximately 90 prepared cores available for analysis, six trees were selected from the Choctawhatchee River to investigate the use of $\delta^{18}O$-depletion in latewood as a proxy for hydroclimate analysis and TC precipitation reconstructions.

2.2. Climate data

At each of these sites (Choctawhatchee, FL, Valdosta, GA, Eglin Airforce Base, FL; Fig. 1), the $\delta^{18}O$ records were compared to numerous climate variables (e.g., precipitation, drought, streamflow, and maximum temperature). To understand precipitation and drought relationships, we selected Climatic Research Unit gridded Time Series v4 (CRU TS) datasets of precipitation and self-calibrating Palmer Drought Severity Index (scPDSI) at 0.5° resolution (Harris et al., 2020). Relationships with maximum temperature were hypothesized to be most important in the hottest months, prompting the selection of summer months (i.e., June, July and August) for inclusion in the analysis.

Streamflow discharge (cubic feet per second) was obtained from USGS Gauge #02366500 near Bruce, located just 1 km upstream from the Choctawhatchee River site (Fig. 1). A linear model was developed based on a nearby Gauge #02361000 in Newton, AL (less than 50 km away from the site) to account for missing data during 1983–1984

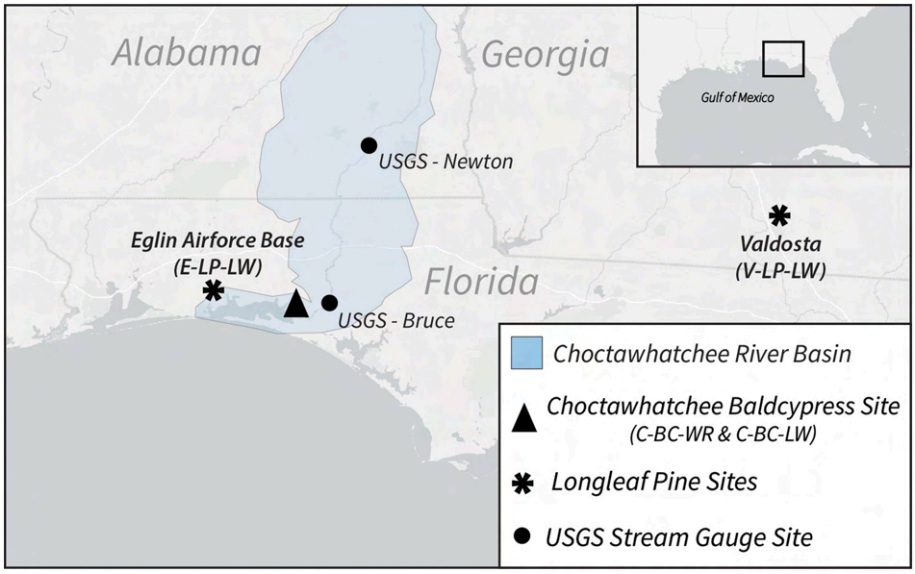

Fig. 1. The Choctawhatchee baldcypress site location (records C-BC-WR, C-BC-LW) and two longleaf pine sites (E-LP-LW, V-LP-LW) used in inter-species comparison. Stream gauge locations within the Choctawhatchee watershed used for streamflow comparisons are identified with circles. (U.S. Geological Survey, 2018), along with the overall Choctawhatchee watershed for comparison.

(Therrell et al., 2020; U.S. Geological Survey, 2023). The mean difference in recorded streamflow between the two gauges was recorded over the entire period of available data and used to estimate streamflow for the Bruce, FL gauge for the two years of missing data (1983–1984).

The total number of statistically significant points of isotopic depletion can be calculated for each site and compared to NOAA's HURDAT2 established record within 223 km of the sample site (World Meteorological Organization's International Best Track Archive for Climate Stewardship, Knapp and Kruk, 2010; Landsea and Franklin, 2013; Matyas, 2010). The Tropical Cyclone Precipitation Database (TCPdat) from Bregy et al. (2019) was used primarily as a point of comparison between the Choctawhatchee, FL Baldcypress site and the Valdosta, GA (V-LP-LW) and Eglin Air Force Base, FL (*E*-LP-LW) longleaf pine sites (Miller et al., 2006; Nelson, 2008). TCPDat is a gridded TC precipitation record spanning 1948–2015, combining the location of historical TC tracks with regional precipitation to determine the amount of TC-related precipitation over a $0.25^{\circ} \times 0.25^{\circ}$ gridded network from June to November. Comparing points of $\delta^{18}O$ depletion to this record allows for interspecies comparison, evaluating the strength of relationships between baldcypress $\delta^{18}O$, longleaf pine $\delta^{18}O$, and TC precipitation. Defining the threshold for isotopic depletion in TC analysis is critical in assessing the relationship between TC activity and baldcypress $\delta^{18}O$. One standard deviation below the series mean ($\sigma \leq -1$) was a natural starting point for determining statistically significant depletion. This initial investigation was unsatisfactory, as years with substantial TC activity displayed strong isotopic depletion relative to the year prior without meeting the ≤ -1 threshold. Increasing the sensitivity of the threshold to that of Miller et al. (2006), Nelson (2008), and Labotka et al. (2016) ($\sigma \leq -0.5$) adds additional years for analysis.

2.3. Tree-ring data

All tree-ring series for this study were crossdated with a previous study (Tucker et al., 2022). Six trees from that previous study (Therrell et al., 2020) were sampled for stable oxygen isotopic analysis. While latewood is generally considered preferable with stable oxygen isotopic analysis, previous work with conifers has successfully used whole-ring samples to compare with hydroclimatic variables, especially when extremely narrow ring-width makes sampling season-wood difficult (Treydte et al., 2007; Weigl et al., 2008; Nagavciuc et al., 2022). As this study represents the first use of the method in the species, we felt that a holistic approach was necessary in preliminary exploration of the proxy. Rather than combining cores from either side of each tree, one core, representing one side of each tree was used. While an isotope chronology developed from four trees is typically considered the minimum for an absolute value reflective of study site conditions (Leavitt and Long, 1984), given limitations on sample core availability and that method testing was supplementary to the overall analysis, two trees for whole-ring analysis were used from the Choctawhatchee site (C-BC-WR) to compare and validate sampling methods relative to latewood (LW) analysis alone.

We compared the data from whole-ring sampling to season-wood sampling. The remaining four trees were selected for latewood (LW) analysis, where the last 1/3 of each annual growth ring was separated with a razor blade (Fig. 2). Because baldcypress often does not produce sufficient LW material for isotopic analysis, two cores from each of the four trees were used, combining 1/3 LW samples for each year from both cores into a single sample. Combining sample material from opposing sides of each tree eliminates circumferential variability, which can otherwise be misinterpreted as climatic response (Leavitt, 2010). This 1/3 LW sampling is also necessary to produce results while simultaneously reducing any intercorrelation between earlywood (EW) and LW

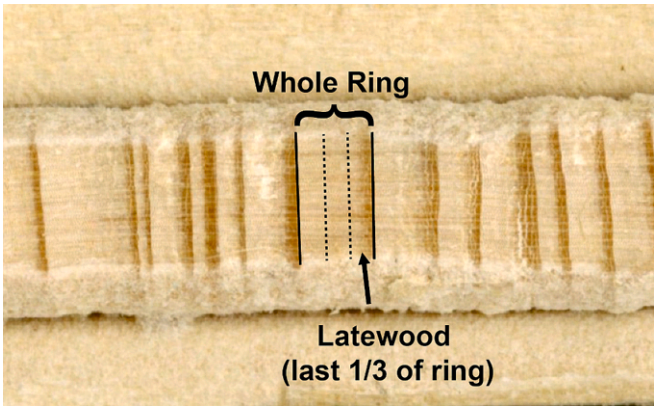

Fig. 2. Core slicing delineations used to develop whole-ring and latewood (LW; last 1/3 of ring) records.

(Therrell et al., 2020). False rings were occasionally found in samples, but this did not change sampling protocol; tree rings were still divided into thirds. In addition, EW that forms after the occurrence of a false ring is likely to have incorporated TC precipitation as source water, making it important for LW analysis despite its light, porous cellular structure (Therrell et al., 2020; Tucker et al., 2022).

Individual rings are sliced with disposable razor blades under a compound microscope and placed in labeled 2.0 mL microtubes to be processed. Sampling with razor blades and a microscope is more affordable and accessible than alternatives such as micro-milling and laser ablation, while also maintaining the precision required to cut along narrow ring boundaries. All trees were sampled at designated ring boundaries beginning with 1960, resulting in 50–60 individual tree rings per sampled tree depending on the original sampling date at each site. All samples were then chemically processed to extract α-cellulose following modified methodology from Leavitt and Danzer (1993). To extract α-cellulose, a bleaching solution composed of sodium chlorite and acetic acid is first applied to the sliced tree rings and allowed to bleach overnight, converting lignin to cellulose. Additional treatments of the bleaching solution are conducted to ensure thorough delignification, which was indicated by a whitening of the sample. Organic components such as resin, oils, and fungus are then removed in 99.9 % ethanol. Next, a 17 % sodium hydroxide solution is applied for 30 min to digest hemicellulose before being neutralized with 10 % hydrochloric acid. A final ethanol soak is used to expedite drying. Samples are placed on a Fisherbrand Mini Vortex Mixer at each step to ensure homogeneity and frequent DI water rinses between treatments minimize chemical cross-contamination. After completely drying, the processed tree-ring α-cellulose is weighed on a Mettler Toledo microbalance. Approximately 400 ± 100 μg of sample material per ring is wrapped in a silver capsule before being sent to the Stable Isotope Laboratory at the University of Arkansas. Here, samples are converted to CO gas with high-temperature degradation (pyrolysis), and results are recorded in per mil notation using Eq. (1),

$$\delta^{18}O = (Rsample/Rstandard - 1) \times 1000 \quad (1)$$

where Rsample is defined as $^{18}O/^{16}O$, and Rstandard as the lab standard, or the Vienna Standard Mean Ocean Water (VSMOW). Results for the 4 trees were pooled (combined) into a single $\delta^{18}O$ record for LW alone at the Choctawhatchee site (hence forth referred to as the C-BC-LW). For comparison, we also accessed data from previous, nearby research on tree-ring $\delta^{18}O$ stable isotopic analysis (e.g., V-LP-LW, E-LP-LW; Miller et al., 2006; Nelson, 2008; Labotka et al., 2016) and directly compared values from these published studies to the findings from this work.

2.4. Statistical methods

For climate and interspecies comparisons (e.g., C-BC-LW, V-LP-LW, E-LP-LW), the z-scores of annual $\delta^{18}O$ are calculated, ensuring comparability without altering correlation coefficients. Minimal autocorrelation identified in autoregressive fit analysis combined with the high rate of water replacement, along with shallow-rooted physiology of baldcypress led us to interpret the z-scores of the $\delta^{18}O$ values directly (Supplemental Fig. 1).

Relationships between the LW $\delta^{18}O$ records (e.g., C-BC-LW, V-LP-LW, E-LP-LW) and precipitation, streamflow, drought and maximum temperature were investigated over varying time intervals using packages “dplr” and “treeclim” within the computing program R (Bunn, 2008; Zang and Biondi, 2015; R Core Team, 2024). Because isotopic values in tree rings are not impacted by age, removing growth trends is unnecessary (Gagen et al., 2008; Young et al., 2011; Duffy et al., 2019). Additionally, climate variables (precipitation, streamflow, self-calibrated Palmer Drought Severity Index, and maximum summer temperature) were analyzed for temporal and spatial relationships using KNMI Climate Explorer (www.climexp.knmi.nl; Trouet and Oldenborgh, 2013), an online application used to test relationships between a host of climate indices and user-uploaded time-series.

3. Results

3.1. Drought

In Fig. 3 we see normalized summer scPDSI (red) and C-BC-LW $\delta^{18}O$ (black). Though these data sets do not match in magnitude through time, 13 years identified as having seasonal drought (i.e., scPDSI $\leqq -0.5$) were categorized by the presence of significant $\delta^{18}O$ enrichment (yellow bars). The drought response in C-BC-LW $\delta^{18}O$ was then compared to that of previously developed longleaf pine $\delta^{18}O$ (e.g., V-LP-LW, E-LP-LW) records to investigate potential differences in species or site-specific water flux. Interspecies comparison of δ18O drought response may be reflective of differences in frontal and TC rainfall water availability, giving valuable insight into differing forest responses after hydroclimatic disturbance. In comparison, species or site-specific phenomena in each $\delta^{18}O$ record can be disentangled from broad-scale drivers of isotopic variation. C-BC-LW $\delta^{18}O$ data indicate stronger spatial correlations with scPDSI than other previously collected data in the region (e.g., V-LP-LW, E-LP-LW; Fig. 4). $\delta^{18}O$ data from V-LP-LW and E-LP-LW have weaker correlations with scPDSI both in their spatial extent and in the value of their correlation coefficients. In these analyses, negative correlation indicates that $\delta^{18}O$ enrichment is consistent with episodic drought.

C-BC-LW $\delta^{18}O$ also shows strong negative correlations with precipitation data alone (Fig. 5). Similarly to PDSI, both correlation coefficients and spatial extent exhibit the strength of these correlations. In comparison analyses to understand the seasonality of tree-ring sampling, C-BC-WR $\delta^{18}O$ and C-BC-LW $\delta^{18}O$ data were compared to precipitation and scPDSI data. C-BC-LW $\delta^{18}O$ exhibited stronger correlations in all analyses. Temporal stability exists for the relationship between LW $\delta^{18}O$ and precipitation (Fig. 6b). Consistently strong negative relationships between both the C-BC-LW and C-BC-WR $\delta^{18}O$ records and precipitation and streamflow are shown throughout the March–July and June–August period.

C-BC-LW $\delta^{18}O$ correlated with streamflow near the site with a ~ 1 month lag in corollary strength is observed between the two parameters, essentially displaying this relationship with atmospheric precipitation before streamflow (Fig. 6a). A weaker, but significant *positive* relationship is identified between C-BC-LW $\delta^{18}O$ and fall precipitation (October, November, December).

Finally, the C-BC-LW $\delta^{18}O$ record demonstrates significant correlations with summer (June, July, August) max temperature (Fig. 7). Despite being centered >200 km north of the Choctawhatchee River basin, the relationship appears over the region at $0.4 < p > 0.5$. Much of this correlation lies along the GC, indicating a response to regional temperature rather than isolated site conditions or fractionation processes occurring on smaller scales. High summer temperatures drive increased rates of soil-water evaporation, driving increased soil fractionation. Similar data interpretation has been used in continental-scale reconstruction of drought and patterns in multi-decadal climate oscillations (Freund et al., 2023; Rodriguez-Caton et al., 2024).

3.2. Tropical cyclones

Of the eight observed $\delta^{18}O$ depletions at or below one standard deviation from the mean (Table 1), only three were associated with TC events making landfall within 223 km of the study site in that respective year (1975, 1989, 1994). However, when considering years that did not quite reach a full standard deviation below the mean but still were associated with large residual depletions from the year prior, we identified 9 out of 13 total years associated with TCs. Included within these additional four years are 1964's Hurricanes Dora and Elda (both Cat 4), 1966's Hurricane Alma (Cat 3), 1975's Hurricane Eloise (Cat 3), and

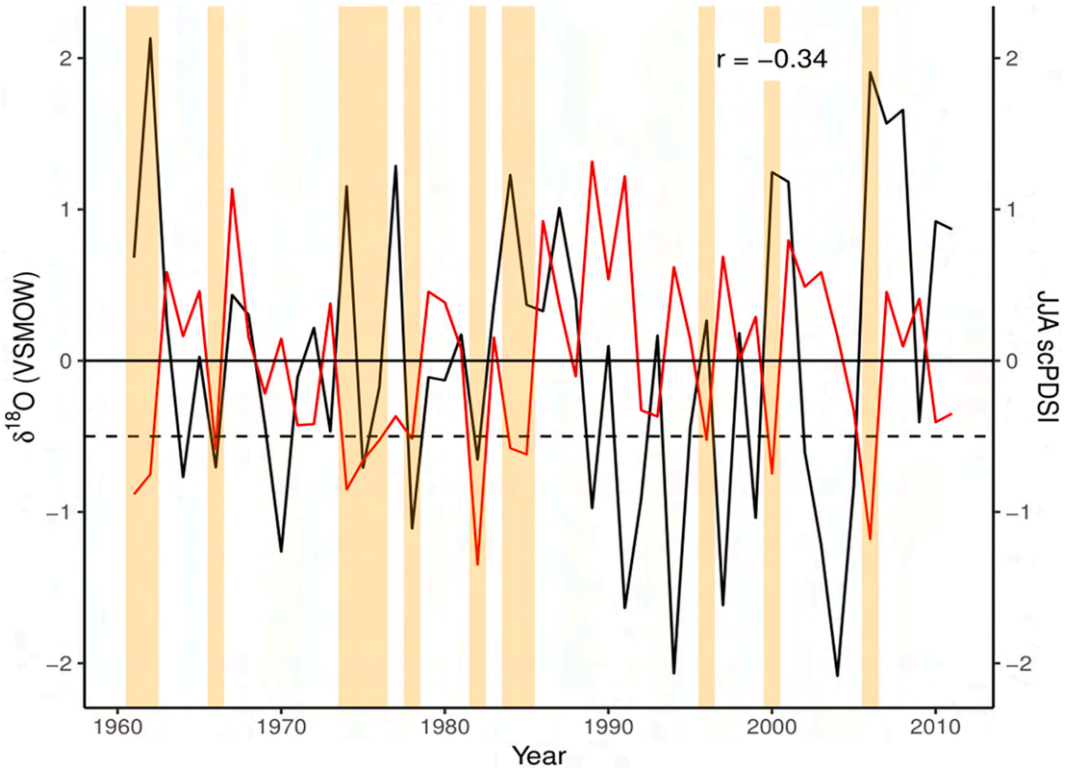

Fig. 3. Summer (June–August) self-calibrating Palmer Drought Severity Index (scPDSI; red) plotted against Choctawhatchee baldcypress (C-BC-LW) LW $\delta^{18}O$ (black). Drought years where scPDSI was identified to have a negative correlation ($r = -0.34$) are included (yellow highlight).

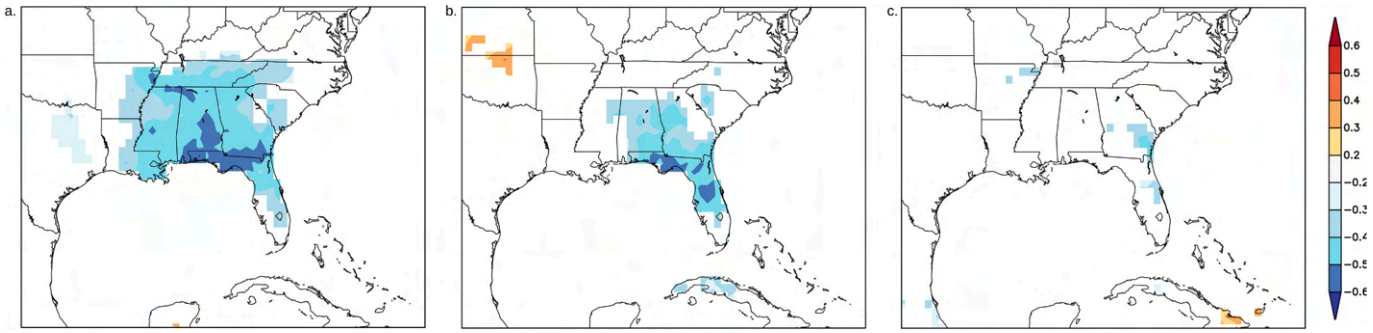

Fig. 4. Summer (June–August) composite correlations between seasonal scPDSI (CRU TSU) and C-BC-LW $\delta^{18}O$ (a., 2.0 % < pfield <5.0 %), V-LP-LW $\delta^{18}O$ (b., 20.0 % < pfield <50.0 %) and E-LP-LW $\delta^{18}O$ (c., 10.0 % < pfield <20.0 %). Results are shown for the recorded overlapping years (1961–1997) with EW + LW years in Nelson.

2009's Hurricane Ida (Cat 2). Several years of TC activity over the site may be related to large ^{18}O depletion events relative to the year prior but never dipped below the $\sigma \leq -0.5$ threshold for significance. To determine whether $\delta^{18}O$ in source-water carries over year-to-year, ^{18}O depletion relative to the year prior was calculated (n1−n0). While a vast majority of years with significantly negative (n1 – n0 < −0.5) relative decreases were also those of significant annual depletion, an additional six years were identified as experiencing significant depletion relative to the previous year. Of these, three were associated with annual TC activity (an unnamed tropical storm in 1969, Elena, Juan, and Kate in 1985, and Claudette and Ida in 2009; Table 1).

Over the 50-year time series for the Choctawhatchee site, a total of 24 years were identified with TCPDat as years in which precipitation from TCs passed over the Choctawhatchee watershed. Significant events have depleted $\delta^{18}O$ with no TC precipitation in the respective year. When comparing the C-BC-LW $\delta^{18}O$ record to the E-LP-LW $\delta^{18}O$ record, the period of analysis was shortened due to the E-LP-LW record ending in 2004. Between 1961 and 2004, both the E-LP-LW and C-BC-LW $\delta^{18}O$ series recorded anomalously low $\delta^{18}O$ during six of the seventeen precipitation-producing TC events from TCPDat. Three of these six events were recorded within the same years between both records, while the remaining three were exclusive to the respective record and site. Four $\delta^{18}O$-depletion/no TC events were recorded in the E-LP-LW $\delta^{18}O$ record, compared to three in the C-BC-LW $\delta^{18}O$ record (Fig. 8).

4. Discussion

4.1. Interspecies comparison

Longleaf pine LW $\delta^{18}O$ (e.g., V-LP-LW, E-LP-LW) have weaker correlations with scPDSI both in their spatial extent and in the value of their correlation coefficients. In explaining differences in drought response between the C-BC-LW, E-LP-LW, and V-LP-LW $\delta^{18}O$ records, a comprehensive understanding of species-specific growth habits and differences

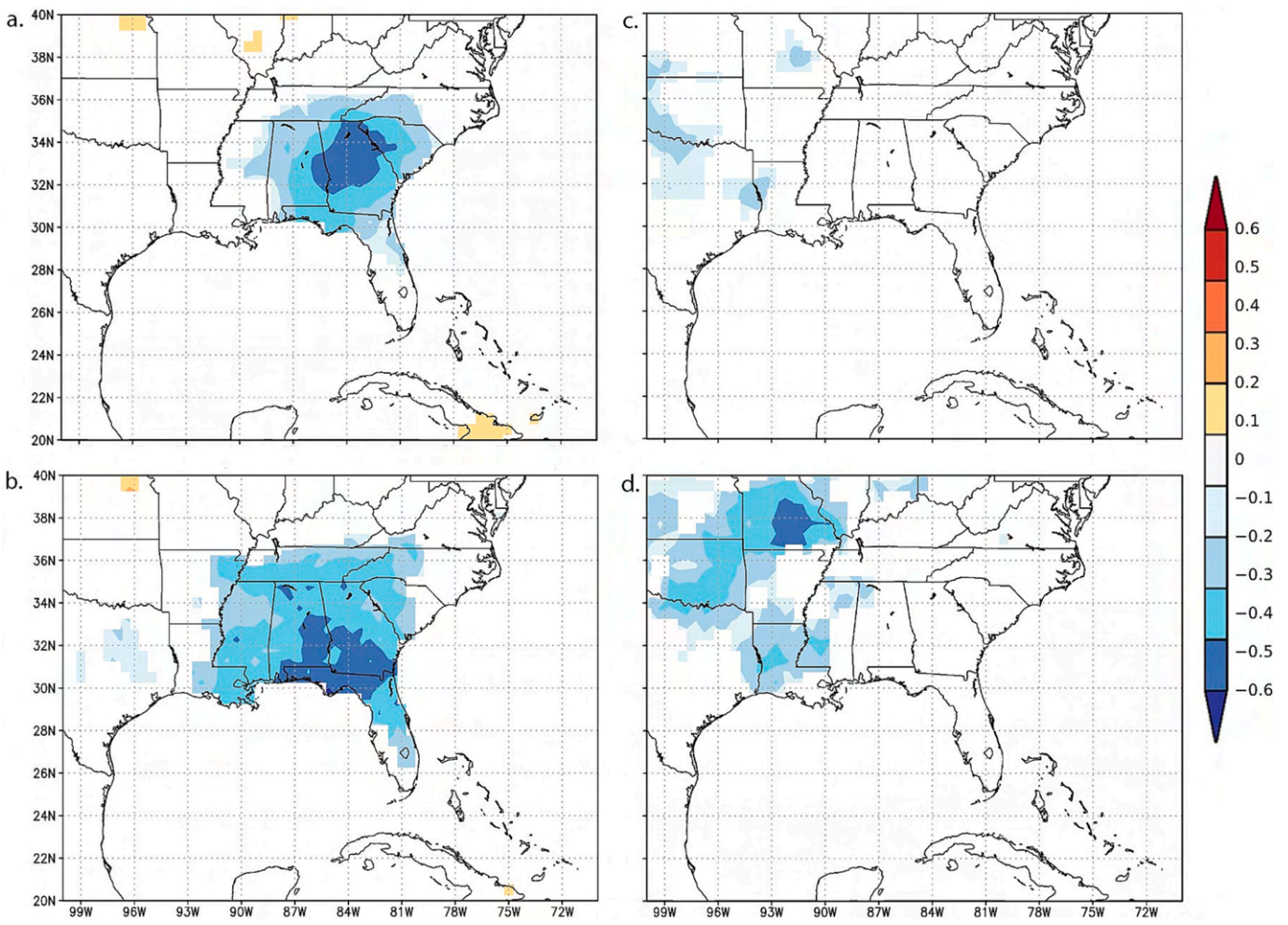

Fig. 5. C-BC-LW $\delta^{18}O$ pooled series (a., b.) and the C-BC-WR $\delta^{18}O$ series (c., d.) correlation to seasonal precipitation (a., c.) and scPDSI (b., d.) in KNMI Climate Explorer (Trouet and Oldenborgh, 2013).

in site conditions is critical. Interspecies variability of tree-ring stable isotopes within similar growth environments is lower than trees of the same species growing in different environments (Leavitt, 2010). While some have noted distinct differences amongst species exposed to the same conditions, the depth of water extraction is hypothesized to be a primary driver in driving interspecies $\delta^{18}O$ variation (Marshall and Monserud, 2006). However, any disparity in fractionation occurring because of a difference in species is minimized in LW sampling, as the shallow root systems of both baldcypress and longleaf pine are predominantly limited to surface water (Stahle et al., 1985a; Stahle et al., 1985b). ^{18}O decreases exponentially with soil depth (Zimmerman et al. 1967). Typical longleaf pine taproots reach 3–5 m below the surface, an adaptation to survive low-intensity fires common in grassland savannas (Heyward, 1933; Addington et al., 2006). While typical vertical growth in baldcypress has not been directly noted, root systems in such wetland trees are typically shallow, penetrating less than 1.5 m into the soil. While the exact percentage of ground versus meteoric water uptake has yet to be quantified, the relatively deeper taproot of longleaf pine provides a potential explanation for such variation in LW $\delta^{18}O$. The sandy, loamy soils typical of longleaf pine sandhills in southern Georgia are well-drained and will remain relatively dry throughout the year, only wetting out during periods of intense rainfall (Labotka et al., 2016). Tree growth in these ecosystems is suddenly spurred by newly available atmospheric water. Conversely, baldcypress trees are reliant on the consistent moisture of waterlogged floodplains of their native range. During periods of drought, growth suppression is observed (Stahle et al., 1985a; Stahle et al., 1985b). Atmospheric precipitation is typically depleted in ^{18}O relative to subsurface and groundwater, as sources of fractionation are limited to evaporative processes in the atmosphere (Clark and Fritz, 1997; Winter et al., 1998; Nyarko et al., 2010). The enrichment of ^{18}O during these same periods is likely explained by decreased rates of groundwater recharge; excess rainfall dilutes surface-water, enriching soil and surface-water with ^{16}O. The opposite is true during periods of drought: Preferential evaporation of ^{16}O amplifies alongside higher temperatures, and decreased rates of surface runoff lead to enriched ^{18}O in surface-water (Tang and Feng, 2001).

Even if relatively minute, evaporative upwelling would contribute an abnormally high percentage of water to the surface during these years, increasing the total amount of fractionation occurring in water utilized by wetland vegetation. The opposite has been observed in fast-draining soils, where isotopic evidence has indicated that atmospheric precipitation is the primary source of soil-water (Kvaerner and Klove, 2006; Kalvans et al., 2020). This provides a potential explanation as to why the sandy, fast-draining soils of southern Georgia are not as conducive to drought reconstruction in longleaf pine $\delta^{18}O$ despite successful precipitation records developed with the proxy (Labotka et al., 2016).

4.2. Drought response

A possible explanation for the observed ^{18}O enrichment during periods of negative scPDSI might be a shift in source-water. Because of drought stress, baldcypress trees may be pulling water originally from

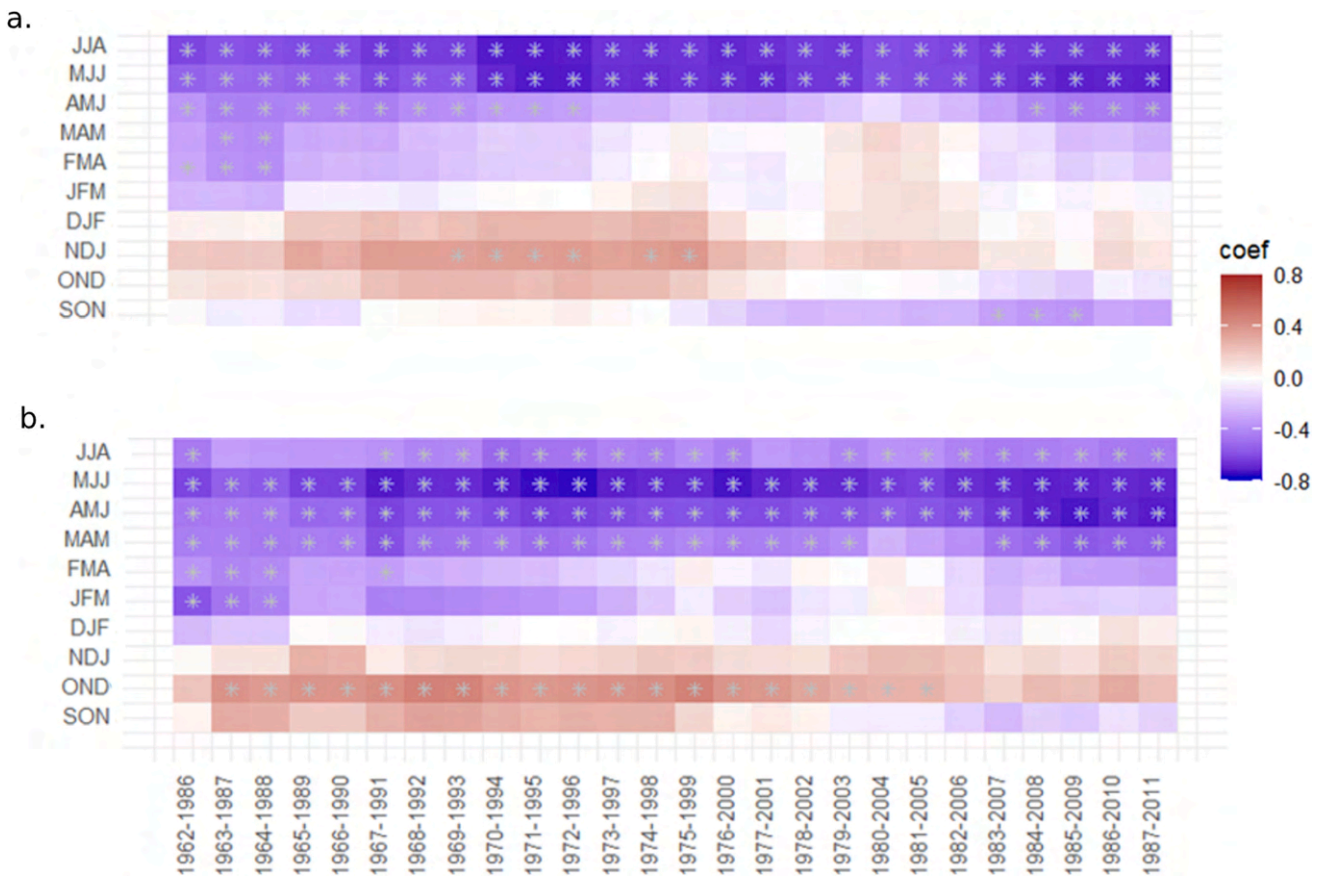

Fig. 6. The correlation between the C-BC-LW $\delta^{18}O$ record and streamflow (a), and precipitation (b) in 25-year moving averages with a confidence interval (CI) of 95 %. Significant correlations at $r \geq 0.4$ between the averaged $\delta^{18}O$ and 3-month average of selected climate indices are marked with asterisks.

increasingly deep places within the soil profile, leaving the water $\delta^{18}O$ drastically altered. Kinetic fractionation occurs within groundwater at a regular rate, with diffusion primarily dependent on water saturation, soil porosity, and atmospheric humidity (Zimmermann et al., 1967; Barnes and Allison, 1988). Groundwater has been shown to constitute the main source of soil-water in wetland environments (Clay et al., 2004; Kalvans et al., 2020). Mature baldcypress trees in coastal environments have been theorized to use some amount of groundwater as a strategy to survive saltwater intrusion (Carmichael et al., 2018). The shallow soil column of the coastal floodplain and deeper rooting may still access water influenced by surface evaporation, preventing the isotopic depletion in $\delta^{18}O$ that is commonly observed when trees switch to deeper, more protected groundwater sources. This means that even during drought, when trees may shift to slightly deeper sources, these water sources remain isotopically enriched. While such research did not note ^{18}O fractionation at the root level, this shift in water source is a possible explanation for the observed drought response.

This correlation is strongest in July–August, with a significance of 2.0 % < pfield <5.0 % and 40–44 % coverage at $p < 0.10$. No significant correlations are observed over the same period between scPDSI and either the V-LP-LW or E-LP-LW records. However, this climate signal is very likely weakened by the reduced sample size, as only years within the 1961–2011 period are shown to ensure the same drought events are displayed between sites. The V-LP-LW and E-LP-LW records end before 2011 (1997 and 2004 respectively), reducing the number of years available in the spatial analysis. While drought response in C-BC-LW $\delta^{18}O$ exceeds the performance of other species, results in this study indicate that more precise methods can produce best results. Even as distinct differences amongst species exposed to the same conditions occur, the depth of water extraction is hypothesized to be a primary driver in driving interspecies $\delta^{18}O$ variation (Marshall and Monserud, 2006). However, any disparity in fractionation occurring because of a difference in species is minimized in LW sampling, as the shallow root systems of both baldcypress and longleaf pine are predominantly limited to surface water (Stahle et al., 1985a; Stahle et al., 1985b). Additionally, the temporal stability of these relationships is present for summer months (June–August; Fig. 6). This trend is expected given the site's location within the drainage basin, near the river mouth of the watershed, as the influx of precipitation will take time to pool at the alluvial catchment where baldcypress trees were sampled.

Previous work also demonstrates significant correlations between baldcypress total ring width and March–July temperature because of seasonal fluctuations in water level and an inverse correlation with precipitation ($r = -0.43$ in June; $r \sim -0.30$ in March–July) (Stahle et al., 1985a; Stahle et al., 1985b; Stahle et al., 2012). The C-BC-LW $\delta^{18}O$ record demonstrates significant correlations with summer (June, July, August) max temperature, as shown in Fig. 7. This relationship further indicates drought as a primary driver of $\delta^{18}O$ enrichment.

Our results suggest that baldcypress exhibits a somewhat anisohydric drought response, shifting its water source to deeper, less available water rather than endure extended periods of stomatal closure. This is a potential product of drought being less common throughout the species' evolutionary history. If baldcypress is using subsurface water during drought periods and displaying clear indications of stress, increasing drought frequency and intensity poses a threat to these ecosystems. The increased risk of hydraulic failure associated with anisohydry during extreme drought presents an elevated conservation concern for baldcypress forests, as these hydric forests may be particularly vulnerable to more frequent and extreme droughts expected under current climate warming (IPCC, 2023; Cook et al., 2022; Moss et al., 2024).

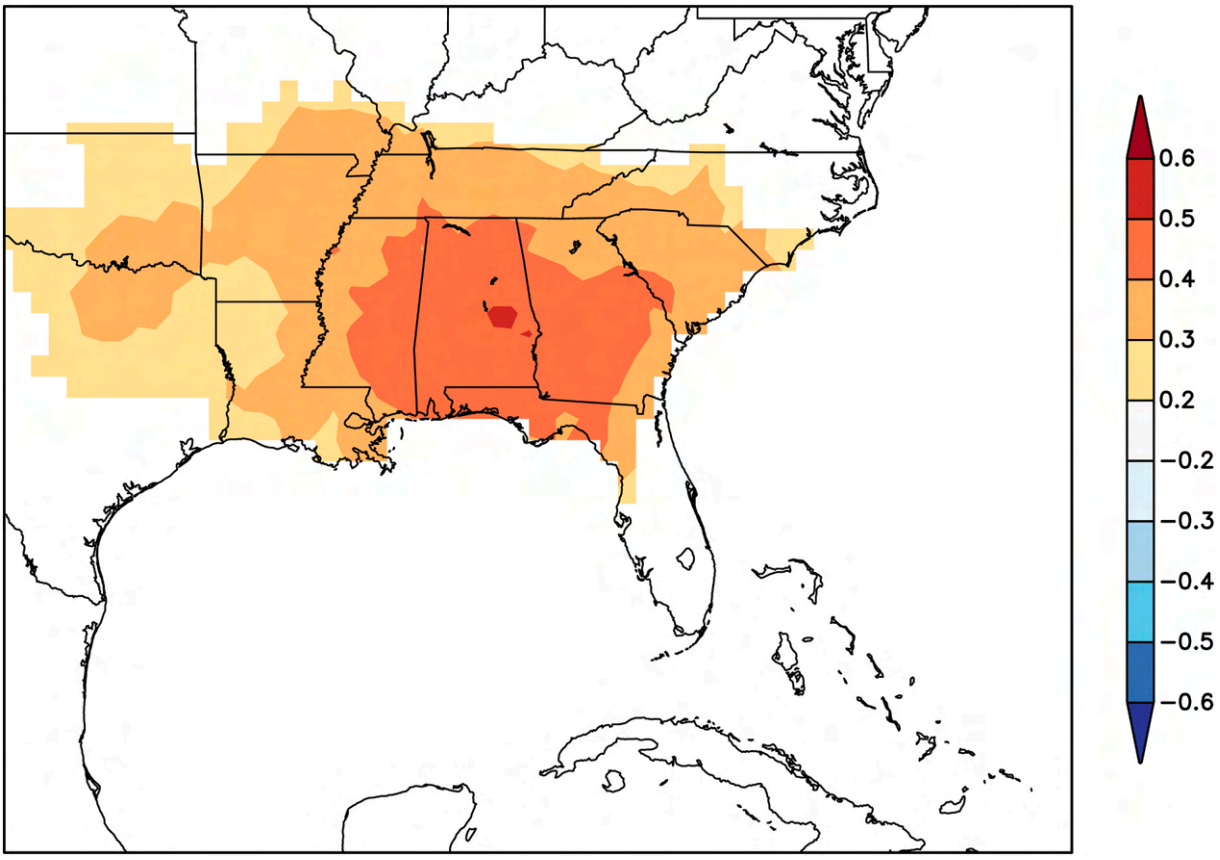

Fig. 7. Spatial correlations between C-BC-LW $\delta^{18}O$ and maximum temperature through the summer (June–August) months (1961–2011). 0.0 % < pfield <0.1 %. Data referenced is sourced from CRU TS (Harris et al., 2020).

4.3. Tropical cyclone response

Baldcypress' past use in studies of southeastern hydroclimate makes it of particular interest for tropical cyclone reconstruction. Tree-ring isotopic records of southeastern TC activity have only been explored in longleaf pine, namely in the two records included within previous climate comparisons (Miller et al., 2006; Nelson, 2008; Labotka et al., 2016). These preliminary studies did not show perfect relationships between tree-ring stable isotopic analysis and tropical cyclone parameters. Likewise, the results of our study are exploratory with respect to tropical cyclone activity and highlight future pathways of exploration for this relationship.

Fractionation within TC spiral rainbands causes isotopic depletion in the storm precipitation, inundating soils with lighter ^{16}O-enriched water. However, if drought conditions are prevalent during years of TC activity, the isotopic depletion may not be captured in the tree rings (Miller et al., 2006; Nelson, 2008; Labotka et al., 2016). Intra-annual growth may incorporate source water from both ^{18}O-enriched subsurface water as well as ^{18}O-depleted TC precipitation, depending on the precise date of TC activity. Years with TC activity over the watershed are displayed alongside their respective scPDSI and normalized C-BC-LW $\delta^{18}O$ value in Supplemental Fig. 2. Past work has demonstrated this same relationship, with Nelson (2008) noting the occurrence of a TC during 6 out of the 11 years when drought conditions were not captured by the $\delta^{18}O$-PDSI comparison. Results from the C-BC-LW $\delta^{18}O$ record seem to indicate that baldcypress $\delta^{18}O$ is more sensitive to summer drought than longleaf pine $\delta^{18}O$ when developing a record of TC activity (Fig. 4). This is consistent with previous work in baldcypress tree-ring width, as the species has produced the most complete paleo records of drought, streamflow, and precipitation in the southeastern United States.

Not all TCs corresponded to $\delta^{18}O$ anomalies. This suggests that significant depletions are being muted by some other climatic anomaly measured in $\delta^{18}O$, as sampling exclusively LW portions of annual rings is specifically practiced to reduce the influence of precipitation from previous years (Leavitt and Szejner, 2022). In addition, three of the low-$\delta^{18}O$/no TC occurred during years (1978, 1991, 1999) in which NOAA's Tropical Cyclone Rainfall database tracked TC-derived precipitation over the watershed, potentially causing the observed depletion events. Tropical Storm Bill made landfall on June 30, 2003 in south-central Louisiana, and passed farther than 223 km of the Choctawhatchee watershed. Similarly on June 26, 1989, Tropical Storm Allison made landfall in eastern Texas also far outside the 223 km buffer used in this study. However, because of their lopsided rain fields, TS Bill and TS Allison produced more than 10 in. and 7 in. of rain over large portions of the watershed. These factors influencing rain within the Choctawhatchee watershed are complex and difficult to quantify but including these two events bring the record to a total of 11/13 TCs associated with LW $\delta^{18}O$ depletion events.

Years 1989 and 2003 also correspond to important marker years in the false-ring record (Therrell et al., 2020; Tucker et al., 2022). False rings (i.e., intra annual density fluctuations) in baldcypress often correspond to summer season high-water events that mimic spring flooding. Added water availability encourages the tree to produce earlywood cells following a period of thicker cell wall growth and these growth aberrations can be seen clearly under a microscope. Previous research indicates that 77 % of these false ring occurrences correspond to TC rainfall (Tucker et al., 2022). Data from Tucker et al. (2022) are included in Fig. 8 as vertical dashed lines. Eight of the 14 false ring events are also LW δ18O depletion events in this study, though not all these years correspond with high TCP events. Though the TCP record is useful for generalizing precipitation within a TC, our results do not

Table 1
Years with year-to-year relative $\delta^{18}O$ depletion z-score ≤ 0.5 and TC category over Choctawhatchee site (C-BC-LW). Intensity is determined by maximum recorded wind speed within 223 km of the site, rather than maximum TC intensity, with Tropical Storms (TS), Hurricanes (H) with Category (Cat) indicated. "NA" indicates no TC over the watershed in the respective year. Years with high false ring (HFR) proportions (⩾20 % of trees exhibiting a false ring) for Choctawhatchee are indicated with an asterisks. Bolded years indicate the 8 events that also had strong $\delta^{18}O$ depletion.

Year	C-BC-LW $\delta^{18}O$ z-score	Difference	HFR	TC category over site
1961	0.680826	–	*	NA
1963	0.262756	−1.8689		NA
1964	−0.76964	−1.03239		Hilda/Dora (Cat 4)
1965	0.025672	–	*	TS 1
1966	−0.70567	−0.73134		Alma (H Cat 3)
1969	−0.42223	−0.72503		Unnamed (TS)
1970	−1.2618	−0.83957		Becky (TS)
1971	−0.10906	–	*	Fern (HS), TS 8
1973	−0.46721	−0.68447		NA
1975	−0.70795	−1.86091	*	Eloise (Cat 3)
1978	−1.10934	−2.39698		NA
1982	−0.65404	−0.82745		NA
1983	0.369791	–	*	NA
1985	0.369335	−0.85863		Elena (Cat 5), Juan (TS)
1987	1.009921	–	*	TS 2
1988	0.407047	−0.60287		NA
1989	−0.97484	−1.38188	*	Allison (TS)
1991	−1.63511	−1.73211		NA
1994	−2.06708	−2.23295	*	Alberto (TS), Beryl (TS)
1997	−1.61699	−1.88338		Danny (Cat 1)
1999	−1.03897	−1.22138		NA
2002	−0.60185	−1.784		Hanna (TS)
2003	−1.21651	−0.61466	*	Bill (TS), Henri (TS)
2004	−2.08393	−0.86741	*	Ivan (Cat 3), Jeanne (TS), Frances (TS)
2005	−0.82544	–	*	Arlene (TS), Cindy (Cat 1), Dennis (Cat 3), Katrina (Cat 3), Rita (Cat 3)
2009	−0.40651	−2.06492		Claudette (TS), Ida (Cat 2)

always align as strongly with TCP as they do with NOAA Tropical Cyclone Rainfall (Roth, 2023). More research is needed to clarify these relationships, and improvement in spatial resolution of tree-ring data sets in this region could improve this understanding.

Differences in drought response are hypothesized to be a result of site/soil characteristics, but differences in depletion events themselves are presently unexplained. Previous research attributed low-$\delta^{18}O$/no TC activity to non-cyclonic rain occurring during El Niño years (Miller et al., 2006; Nelson, 2008; Labotka et al., 2016). As a result of the jet stream shifting southward during these years, increased precipitation with source water originating in latitudes farther north will track over the southeastern United States. This frontal precipitation travels increased distances from its source relative to precipitation during La Niña years, driving further fractionation. The Southern Oscillation Index (SOI) is a measure of large-scale atmospheric pressure fluctuations across the Pacific and is commonly used to quantify the strength of El Niño and La Niña episodes. After accounting for the 2003 $\delta^{18}O$ depletion's association with Hurricane Bill, late-summer SOI values were compared to the remaining low-$\delta^{18}O$/no TC depletion events in the Choctawhatchee record to try to explain these anomalies. Three of these six low-$\delta^{18}O$ years were associated with anomalously strong El Niño episodes ranging between July and September (1982, 1991, and 1992 SOI ≤ -1). While this may be insufficient to indicate a causal relationship between the two, strong El Niño during years of low $\delta^{18}O$ and no regional TC activity is yet another potential explanation for the observed isotopic depletion in the developed record.

When collating these "false positive" detections and missed TC years in the $\delta^{18}O$ record, TC and heavy rainfall events during summer months become important. These results are consistent with results from previous studies of baldcypress false ring analysis (Therrell et al., 2020; Tucker et al., 2022). Unusually high streamflow during the months of June and July correspond to high false ring production and likely aberrations in LW $\delta^{18}O$. For example, during the years 1989 and 2003, Tropical Storms Allison and Bill respectively correspond with high streamflow on the Choctawhatchee River in July. Though these events are not captured in the TCPdat dataset for our study because they are outside of the 223 km buffer used, summer hydroclimate variability is clearly important to baldcypress ring-width, false ring production, and LW $\delta^{18}O$ isotopic composition.

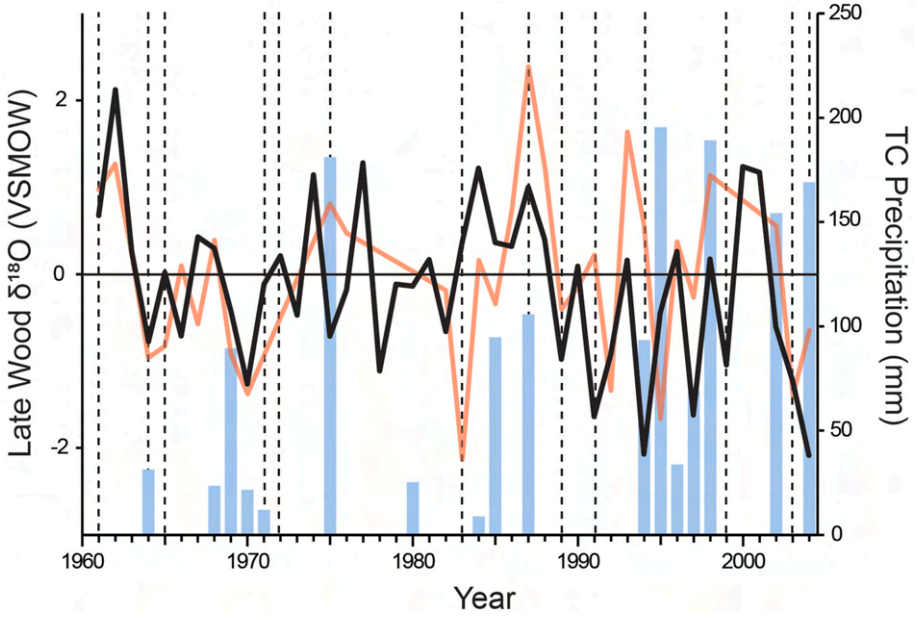

Fig. 8. Comparison of LW $\delta^{18}O$ z-scores to TCPDat (blue) between C-BC-LW (black) and E-LP-LW (red). High false ring years (as interpreted from Therrell et al., 2020 and Tucker et al., 2022) for the Choctawhatchee site are indicated by the vertical black dotted lines. TCPDat indicates precipitation occurring within 223 km of the Choctawhatchee study site, filtered by HURDAT2's storm track and seasonality.

5. Conclusion

This exploratory study examined the use of baldcypress oxygen isotopes for southeastern U.S. hydroclimatic analyses. Results indicate that baldcypress isotopic composition should be explored further as a proxy of hydroclimate in the region, especially as those climate parameters relate to drought. Results of this study indicate that isotopic analysis of baldcypress tree-ring data show similar results and stronger relationships with climatic variables than longleaf pine isotopic analysis. Baldcypress $\delta^{18}O$ analysis has stronger correlations with scPDSI both in spatial extent and in the strength of correlation coefficients than results of previous studies exploring the same in longleaf pine. However, our study sites do not undergo the same site-specific environmental conditions as these previous studies. Future research should expand upon relationships of baldcypress and longleaf pine hydroclimatic relationships.

Strongest hydroclimatic relationships with baldcypress $\delta^{18}O$ exist in extreme values. During these events, baldcypress $\delta^{18}O$ shows potential in tracing tree source-water seasonally, providing insight into temporal and spatial variability in the southeastern floodplain water budget. Though root-depth limitations make baldcypress an unlikely candidate for such analysis, our results indicate that baldcypress' threshold for an interpretable drought stress is lower than that of other species in the region. Additionally, strongest hydroclimatic relationships with baldcypress $\delta^{18}O$ exist in extreme values, and this proxy can produce paleorecords of precipitation, streamflow, drought, maximum summer temperature with a single dataset. Despite an overall lower correlation than ring-width analysis (scPDSI with baldcypress ring-width was calculated to be $r = 0.67$ in Stahle et al., 1998), clear mechanistic explanations uphold climate interpretability with the developed $\delta^{18}O$ record. While the method is used to reconstruct similar hydroclimatic extremes to ring width, $\delta^{18}O$ allows us to directly study water source allocation rather than an indirect archive of tree-growth. Future research may also assess the relationship between tree-ring $\delta^{18}O$ and $\delta^{13}C$, as relationships between the two variables have been shown to affect the photosynthetic process. Depleted $\delta^{18}O$ values could occur with an acceleration of the photosynthetic process or with high stomatal conductance. Sheidegger et al. (2000) produced a model for deriving carbon water relations, and this model may be useful for tree-ring research as well.

In addition to relationships with drought parameters, our results show the versatility of $\delta^{18}O$ analysis in baldcypress with respect to event-based climatic variables, and additional work is justified in order to adequately answer questions surrounding the use of the proxy in reconstructing historical TCs. Results of this study indicate that TC occurrences are captured by baldcypress $\delta^{18}O$, but this signal may be clouded by other environmental factors, especially those related to drought. Additional work is needed to decouple the drought-induced enrichment and TC-induced depletion of baldcypress $\delta^{18}O$ to optimize the proxy for historical TC reconstruction.

CRediT authorship contribution statement

Jared M. Friedman: Writing – review & editing, Writing – original draft, Visualization, Methodology, Investigation, Formal analysis, Data curation, Conceptualization. **Emily A. Elliott:** Writing – review & editing, Visualization, Supervision, Resources, Project administration, Investigation, Funding acquisition, Conceptualization. **Clay S. Tucker:** Writing – review & editing, Supervision, Project administration, Methodology, Investigation, Funding acquisition, Conceptualization. **Joshua C. Bregy:** Writing – review & editing, Methodology, Investigation, Funding acquisition, Data curation, Conceptualization. **Matthew D. Therrell:** Writing – review & editing, Funding acquisition, Data curation, Conceptualization. **Jessie K. Pearl:** Writing – review & editing, Funding acquisition, Conceptualization.

Declaration of competing interest

The authors declare that they have no known competing financial interests or personal relationships that could have appeared to influence the work reported in this paper.

Acknowledgements

This study was primarily funded by the National Science Foundation Paleo Perspectives on Climate Change (NSF P2C2; award #2103115). Initial funding used in preliminary work was acquired through the University of Alabama CARSCA. Thank you to Erik Pollock at the University of Arkansas Stable Isotope and Trace Element Facilities for mass spectrometry of our samples. Thank you to Joe Lambert at The University of Alabama for allowing us access to his facilities during sample preparation. Thank you to Adam Csank for his guidance in acquiring the equipment needed for cellulose processing. Thank you to the numerous undergraduate students who assisted with sample preparation, including Maddie Cherry, Brett Walker, Gabby Abashian, Katy Uptain, and Kira English.

Appendix A. Supplementary data

Supplementary data to this article can be found online at https://doi.org/10.1016/j.scitotenv.2025.180392.

Data availability

Data will be made available on request.

References

Addington, R.N., Donovan, L.A., Mitchell, R.J., Vose, J.M., Pecot, S.D., Jack, S.B., Hacke, U.G., Sperry, J.S., Oren, R., 2006. Adjustments in hydraulic architecture of Pinus palustris maintain similar stomatal conductance in xeric and Mesic habitats. Plant Cell Environ. 29, 535–545. https://doi.org/10.1111/j.1365-3040.2005.01430.x.

Altman, J., Saurer, M., Dolezal, J., Maredova, N., Song, J.-S., Ho, C.-H., Treydte, K., 2021. Large volcanic eruptions reduce landfalling tropical cyclone activity: evidence from tree rings. Sci. Total Environ. 775, 145899. https://doi.org/10.1016/j.scitotenv.2021.145899.

Anderson, S., Ogle, R., Tootle, G., Oubeidillah, A., 2019. Tree-ring reconstructions of streamflow for the Tennessee valley. Hydrology 6, 34. https://doi.org/10.3390/hydrology6020034.

Andreu-Hayles, L., Lévesque, M., Guerrieri, R., Siegwolf, R.T.W., Körner, C., 2022. Limits and strengths of tree-ring stable isotopes. In: Siegwolf, R.T.W., Brooks, J.R., Roden, J., Saurer, M. (Eds.), Stable Isotopes in Tree Rings: Inferring Physiological, Climatic and Environmental Responses, Tree Physiology. Springer International Publishing, Cham, pp. 399–428. https://doi.org/10.1007/978-3-030-92698-4_14.

Barbour, M.M., Walcroft, A.S., Farquhar, G.D., 2002. Seasonal variation in δ13C and δ18O of cellulose from growth rings of Pinus radiata. Plant Cell Environ. 25, 1483–1499. https://doi.org/10.1046/j.0016-8025.2002.00931.x.

Barnes, C.J., Allison, G.B., 1988. Tracing of water movement in the unsaturated zone using stable isotopes of hydrogen and oxygen. J. Hydrol. 100, 143–176. https://doi.org/10.1016/0022-1694(88)90184-9.

Belmecheri, S., Wright, W.E., Szejner, P., Morino, K.A., Monson, R.K., 2018. Carbon and oxygen isotope fractionations in tree rings reveal interactions between cambial phenology and seasonal climate. Plant Cell Environ. 41, 2758–2772. https://doi.org/10.1111/pce.13401.

Bräuning, A., De Ridder, M., Zafirov, N., García-González, I., Petrov Dimitrov, D., Gärtner, H., 2016. Tree-ring features: indicators of extreme event impacts. IAWA J. 37 (2), 206–231. https://doi.org/10.1163/22941932-20160131.

Bregy, J.C., Maxwell, J.T., Robeson, S.M., Ortegren, J.T., Soulé, P.T., Knapp, P.A., 2019. Spatiotemporal variability of tropical cyclone precipitation using a high-resolution, gridded (0.25° × 0.25°) dataset for the eastern United States, 1948–2015. J. Clim. 33, 1803–1819. https://doi.org/10.1175/JCLI-D-18-0885.1.

Bregy, J.C., Maxwell, J.T., Robeson, S.M., Harley, G.L., Elliott, E.A., Heeter, K.J., 2022. US Gulf Coast tropical cyclone precipitation influenced by volcanism and the North Atlantic subtropical high. Commun Earth Environ 3, 164. https://doi.org/10.1038/s43247-022-00494-7.

Brienen, R.J.W., Helle, G., Pons, T.L., Guyot, J.-L., Gloor, M., 2012. Oxygen isotopes in tree rings are a good proxy for Amazon precipitation and El Niño-southern oscillation variability. Proc. Natl. Acad. Sci. 109, 16957–16962. https://doi.org/10.1073/pnas.1205977109.

Bunn, A.G., 2008. A dendrochronology program library in R (dplR). Dendrochronologia 26, 115–124. https://doi.org/10.1016/j.dendro.2008.01.002.

Bureau, U.C., 2019. Coastline America [WWW Document]. Census.gov. URL. https://www.census.gov/library/visualizations/2019/demo/coastline-america.html (accessed 9.17.23).
Burk, R.L., Stuiver, M., 1981. Oxygen isotope ratios in trees reflect mean annual temperature and humidity. Science 211, 1417–1419. https://doi.org/10.1126/science.211.4489.1417.
Carmichael, M., White, J., Smith, W., 2018. Water source utilization in Taxodium distichum (L.) rich. (baldcypress) over the course of a growing season in a restored coastal freshwater wetland vulnerable to saltwater incursion. Castanea 83, 272–287. https://doi.org/10.2179/18-158.
Clark, I., Fritz, P., 1997. Environmental isotopes in hydrogeology. In: [WWW document]. URL. https://www.taylorfrancis.com/pdfviewer/. accessed 9.28.23.
Clay, A., Bradley, C., Gerrard, A.J., Leng, M.J., 2004. Using stable isotopes of water to infer wetland hydrological dynamics. Hydrol. Earth Syst. Sci. 8, 1164–1173. https://doi.org/10.5194/hess-8-1164-2004.
Cook, E.R., Meko, D.M., Stahle, D.W., Cleaveland, M.K., 1999. Drought Reconstructions for the Continental United States.
Cook, E.R., Woodhouse, C.A., Eakin, C.M., Meko, D.M., Stahle, D.W., 2004. Long-term aridity changes in the Western United States. Science 306, 1015–1018. https://doi.org/10.1126/science.1102586.
Cook, B.I., Ault, T.R., Smerdon, J.E., 2015. Unprecedented 21st century drought risk in the American southwest and Central Plains. Sci. Adv. 1, e1400082. https://doi.org/10.1126/sciadv.1400082.
Cook, B.I., Smerdon, J.E., Cook, E.R., Williams, A.P., Anchukaitis, K.J., Mankin, J.S., Allen, K., Andreu-Hayles, L., Ault, T.R., Belmecheri, S., Coats, S., Coulthard, B., Fosu, B., Grierson, P., Griffin, D., Herrera, D.A., Ionita, M., Lehner, F., Leland, C., Marvel, K., Morales, M.S., Mishra, V., Ngoma, J., Nguyen, H.T.T., O'Donnell, A., Palmer, J., Rao, M.P., Rodriguez-Caton, M., Seager, R., Stahle, D.W., Stevenson, S., Thapa, U.K., Varuolo-Clarke, A.M., Wise, E.K., 2022. Megadroughts in the common era and the Anthropocene. Nat Rev Earth Environ 3, 741–757. https://doi.org/10.1038/s43017-022-00329-1.
Copenheaver, C.A., Matiuk, J.D., Nolan, L.J., Franke, M.E., Block, P.R., Reed, W.P., Kidd, K.R., Martini, G., 2017. False ring formation in bald cypress (Taxodium distichum). Wetlands 37, 1037–1044. https://doi.org/10.1007/s13157-017-0938-9.
Dansgaard, W., 1964. Stable isotopes in precipitation. Tellus 16, 436–468. https://doi.org/10.3402/tellusa.v16i4.8993.
Dawson, T.E., 1993. 30 - water sources of plants as determined from xylem-water isotopic composition: Perspectives on plant competition, distribution, and water relations. In: Ehleringer, J.R., Hall, A.E., Farquhar, G.D. (Eds.), Stable Isotopes and Plant Carbon-Water Relations. Academic Press, San Diego, pp. 465–496. https://doi.org/10.1016/B978-0-08-091801-3.50040-4.
Dawson, T.E., Ehleringer, J.R., 1991. Streamside trees that do not use stream water. Nature 350, 335–337. https://doi.org/10.1038/350335a0.
Desantis, L.R.G., Bhotika, S., Williams, K., Putz, F.E., 2007. Sea-level rise and drought interactions accelerate forest decline on the Gulf coast of Florida, USA. Glob. Chang. Biol. 13, 2349–2360. https://doi.org/10.1111/j.1365-2486.2007.01440.x.
Duffy, J.E., McCarroll, D., Loader, N.J., Young, G.H.F., Davies, D., Miles, D., Bronk Ramsey, C., 2019. Absence of age-related trends in stable oxygen isotope ratios from oak tree rings. Glob. Biogeochem. Cycles 33, 841–848. https://doi.org/10.1029/2019GB006195.
Edwards, T.W.D., Aravena, R.O., Fritz, P., Morgan, A.V., 1985. Interpreting paleoclimate from l8O and 2H in plant cellulose: comparison with evidence from fossil insects and relict permafrost in southwestern Ontario. Can. J. Earth Sci. 22, 1720–1726. https://doi.org/10.1139/e85-180.
Epstein, S., Thompson, P., Yapp, C.J., 1977. Oxygen and hydrogen isotopic ratios in plant cellulose. Science 198, 1209–1215.
Feng, X., Epstein, S., 1994. Climatic implications of an 8000-year hydrogen isotope time series from bristlecone pine trees. Science 265, 1079–1081. https://doi.org/10.1126/science.265.5175.1079.
Freund, M.B., Helle, G., Balting, D.F., Ballis, N., Schleser, G.H., Cubasch, U., 2023. European tree-ring isotopes indicate unusual recent hydroclimate. Commun. Earth Environ. 4, 1–8. https://doi.org/10.1038/s43247-022-00648-7.
Gagen, M., McCarroll, D., Robertson, I., Loader, N.J., Jalkanen, R., 2008. Do tree ring $\delta^{13}C$ series from Pinus sylvestris in northern Fennoscandia contain long-term non-climatic trends? Chemical Geology, Stable Isotope Analysis of Tree Rings 252, 42–51. https://doi.org/10.1016/j.chemgeo.2008.01.013.
Gedzelman, S.D., Arnold, R., 1994. Modeling the isotopic composition of precipitation. J. Geophys. Res. Atmos. 99, 10455–10471. https://doi.org/10.1029/93JD03518.
Gessler, A., Ferrio, J.P., Hommel, R., Treydte, K., Werner, R.A., Monson, R.K., 2014. Stable isotopes in tree rings: towards a mechanistic understanding of isotope fractionation and mixing processes from the leaves to the wood. Tree Physiol. 34, 796–818. https://doi.org/10.1093/treephys/tpu040.
Gornitz, V.M., Daniels, R.C., White, T.W., Birdwell, K.R., 1994. The development of a coastal risk assessment database: vulnerability to sea-level rise in the U.S. southeast. J. Coast. Res. 327–338.
Harris, I., Osborn, T.J., Jones, P., Lister, D., 2020. Version 4 of the CRU TS monthly high-resolution gridded multivariate climate dataset. Sci. Data 7, 109. https://doi.org/10.1038/s41597- 020-0453-3.
Heyward, F., 1933. The root system of longleaf pine on the Deep Sands of Western Florida. Ecology 14, 136–148. https://doi.org/10.2307/1932880.
Hsueh, Y.-H., Chambers, J.L., Krauss, K.W., Allen, S.T., Keim, R.F., 2016. Hydrologic exchanges and baldcypress water use on deltaic hummocks, Louisiana, USA. Ecohydrology 9, 1452–1463. https://doi.org/10.1002/eco.1738.
IPCC, 2023. In: Core Writing Team, Lee, H., Romero, J. (Eds.), Climate Change 2023. Synthesis Report. Contribution of Working Groups I, II and III to the Sixth Assessment Report of the Intergovernmental Panel on Climate Change. IPCC, Geneva, Switzerland, pp. 35–115. https://doi.org/10.59327/IPCC/AR6-9789291691647.
Kalvāns, A., Dēliņa, A., Babre, A., Popovs, K., 2020. An insight into water stable isotope signatures in temperate catchment. J. Hydrol. 582, 124442. https://doi.org/10.1016/j.jhydrol.2019.124442.
Keim, B.D., Muller, R.A., Stone, G.W., 2007. Spatiotemporal patterns and return periods of tropical storm and hurricane strikes from Texas to Maine. J. Clim. 20, 3498–3509. https://doi.org/10.1175/JCLI4187.1.
King, K.E., Cook, E.R., Anchukaitis, K.J., Cook, B.I., Smerdon, J.E., Seager, R., Harley, G. L., Spei, B., 2024a. Increasing prevalence of hot drought across western North America since the 16th century. Sci. Adv. 10, eadj4289. https://doi.org/10.1126/sciadv.adj4289.
King, K.E., Harley, G.L., Maxwell, J.T., Rayback, S., Cook, E., Maxwell, R.S., Rochner, M. L., Bergan, E.V., Foley, Z., Therrell, M., Bregy, J., 2024b. Reconstructed late summer maximum temperatures for the southeastern United States from tree-ring blue intensity. Geophys. Res. Lett. 51, e2024GL109099. https://doi.org/10.1029/2024GL109099.
Knapp, K.R., Kruk, M.C., 2010. Quantifying interagency differences in tropical cyclone best-track wind speed estimates. Mon. Weather Rev. 138, 1459–1473. https://doi.org/10.1175/2009MWR3123.1.
Knapp, P.A., Maxwell, J.T., Soulé, P.T., 2016. Tropical cyclone rainfall variability in coastal North Carolina derived from longleaf pine (Pinus palustris mill.): AD 1771–2014. Clim. Chang. 135, 311–323. https://doi.org/10.1007/s10584-015-1560-6.
Knapp, P.A., Soulé, P.T., Maxwell, J.T., Ortegren, J.T., Mitchell, T.J., 2021. Tropical cyclone precipitation regimes since 1750 and the great suppression of 1843–1876 along coastal North Carolina, USA. Int. J. Climatol. 41, 200–210. https://doi.org/10.1002/joc.6615.
Knutson, T.R., Tuleya, R.E., 2004. Impact of CO2-induced warming on simulated hurricane intensity and precipitation: sensitivity to the choice of climate model and convective parameterization. J. Clim. 17, 3477–3495. https://doi.org/10.1175/1520-0442(2004)017<3477:IOCWOS>2.0.CO;2.
Knutson, T., Camargo, S.J., Chan, J.C.L., Emanuel, K., Ho, C.-H., Kossin, J., Mohapatra, M., Satoh, M., Sugi, M., Walsh, K., Wu, L., 2020. Tropical Cyclones and Climate Change Assessment: Part II: Projected Response to Anthropogenic Warming. https://doi.org/10.1175/BAMS-D-18-0194.1.
Kolker, A.S., Allison, M.A., Hameed, S., 2011. An evaluation of subsidence rates and sea-level variability in the northern Gulf of Mexico. Geophys. Res. Lett. 38. https://doi.org/10.1029/2011GL049458.
Kuwayama, Y., Thompson, A., Bernknopf, R., Zaitchik, B., Vail, P., 2019. Estimating the impact of drought on agriculture using the U.S. drought monitor. Am. J. Agric. Econ. 101, 193–210. https://doi.org/10.1093/ajae/aay037.
Kværner, J., Kløve, B., 2006. Tracing sources of summer streamflow in boreal headwaters using isotopic signatures and water geochemical components. J. Hydrol. 331, 186–204. https://doi.org/10.1016/j.jhydrol.2006.05.008.
Labotka, D.M., Grissino-Mayer, H.D., Mora, C.I., Johnson, E.J., 2016. Patterns of moisture source and climate variability in the southeastern United States: a four-century seasonally resolved tree-ring oxygen-isotope record. Clim. Dyn. 46, 2145–2154. https://doi.org/10.1007/s00382-015-2694-y.
Landsea, C.W., Franklin, J.L., 2013. Atlantic hurricane database uncertainty and presentation of a new database format. Mon. Weather Rev. 141, 3576–3592. https://doi.org/10.1175/MWR-D-12-00254.1.
Lawrence, J.R., 1998. Isotopic spikes from tropical cyclones in surface waters: opportunities in hydrology and paleoclimatology. Chem. Geol. 144, 153–160. https://doi.org/10.1016/S0009-2541(97)00090-9.
Lawrence, R.J., Gedzelman, D.S., 1996. Low stable isotope ratios of tropical cyclone rains. Geophys. Res. Lett. 23, 527–530. https://doi.org/10.1029/96GL00425.
Lawrence, J.R., Gedzelman, S.D., Gamache, J., Black, M., 2002. Stable isotope ratios: hurricane Olivia. J. Atmos. Chem. 41, 67–82. https://doi.org/10.1023/A:1013808530364.
Leavitt, S.W., 2010. Tree-ring c–h–o isotope variability and sampling. Sci. Total Environ. 408, 5244–5253. https://doi.org/10.1016/j.scitotenv.2010.07.057.
Leavitt, S.W., Danzer, S.R., 1993. Method for batch processing small wood samples to holocellulose for stable-carbon isotope analysis. Anal. Chem. 65, 87–89. https://doi.org/10.1021/ac00049a017.
Leavitt, S.W., Long, A., 1984. Sampling strategy for stable carbon isotope analysis of tree rings in pine. Nature 311, 145–147. https://doi.org/10.1038/311145a0.
Leavitt, S.W., Szejner, P., 2022. Intra-annual tree-ring isotope variations: do they occur when environment remains constant? Trees 36, 865–868. https://doi.org/10.1007/s00468-022-02304-1.
Lewis, D.B., Finkelstein, D.B., Grissino-Mayer, H.D., Mora, C.I., Perfect, E., 2011. A multitree perspective of the tree ring tropical cyclone record from longleaf pine (Pinus palustris mill.), big thicket National Preserve, Texas, United States. J. Geophys. Res. G: Biogeosciences 116. https://doi.org/10.1029/2009JG001194.
Li, Z.-H., Labbé, N., Driese, S.G., Grissino-Mayer, H.D., 2011. Micro-scale analysis of tree-ring δ18O and δ13C on α-cellulose spline reveals high-resolution intra-annual climate variability and tropical cyclone activity. Chem. Geol. 284, 138–147. https://doi.org/10.1016/j.chemgeo.2011.02.015.
Mann, M.E., Rutherford, S., Wahl, E., Ammann, C., 2007. Robustness of proxy-based climate field reconstruction methods. J. Geophys. Res. Atmos. 112. https://doi.org/10.1029/2006JD008272.
Mann, M., Woodruff, J., Donnelly, J., Zhang, Z., 2009. Atlantic hurricanes and climate over the past 1,500 years. Nature 460, 880–883. https://doi.org/10.1038/nature08219.

Manuel, J., 2008. Drought in the Southeast: lessons for water management. Environ. Health Perspect. 116 (4) [WWW Document]. URL. https://ehp.niehs.nih.gov/doi/full/10.1289/ehp.116-a168 (accessed 12.19.23).
Margolis, E.Q., Guiterman, C.H., Chavardès, R.D., Coop, J.D., Copes-Gerbitz, K., Dawe, D.A., Falk, D.A., Johnston, J.D., Larson, E., Li, H., Marschall, J.M., Naficy, C. E., Naito, A.T., Parisien, M.-A., Parks, S.A., Portier, J., Poulos, H.M., Robertson, K.M., Speer, J.H., Stambaugh, M., Swetnam, T.W., Tepley, A.J., Thapa, I., Allen, C.D., Bergeron, Y., Daniels, L.D., Fulé, P.Z., Gervais, D., Girardin, M.P., Harley, G.L., Harvey, J.E., Hoffman, K.M., Huffman, J.M., Hurteau, M.D., Johnson, L.B., Lafon, C. W., Lopez, M.K., Maxwell, R.S., Meunier, J., North, M., Rother, M.T., Schmidt, M.R., Sherriff, R.L., Stachowiak, L.A., Taylor, A., Taylor, E.J., Trouet, V., Villarreal, M.L., Yocom, L.L., Arabas, K.B., Arizpe, A.H., Arseneault, D., Tarancón, A.A., Baisan, C., Bigio, E., Biondi, F., Cahalan, G.D., Caprio, A., Cerano-Paredes, J., Collins, B.M., Dey, D.C., Drobyshev, I., Farris, C., Fenwick, M.A., Flatley, W., Floyd, M.L., Gedalof, Z., Holz, A., Howard, L.F., Huffman, D.W., Iniguez, J., Kipfmueller, K.F., Kitchen, S.G., Lombardo, K., McKenzie, D., Merschel, A.G., Metlen, K.L., Minor, J., O'Connor, C.D., Platt, L., Platt, W.J., Saladyga, T., Stan, A.B., Stephens, S., Sutheimer, C., Touchan, R., Weisberg, P.J., 2022. The North American tree-ring fire-scar network. Ecosphere 13, e4159. https://doi.org/10.1002/ecs2.4159.
Marshall, J.D., Monserud, R.A., 2006. Co-occurring species differ in tree-ring δ18O trends. Tree Physiol. 26, 1055–1066. https://doi.org/10.1093/treephys/26.8.1055.
Mattoon, W., 1915. The Southern Cypress. United States Department of Agriculture.
Matyas, C.J., 2010. Associations between the size of hurricane rain fields at landfall and their surrounding environments. Meteorog. Atmos. Phys. 106, 135–148. https://doi.org/10.1007/s00703-009-0056-1.
Maxwell, J.T., Bregy, J.C., Robeson, S.M., Knapp, P.A., Soulé, P.T., Trouet, V., 2021. Recent increases in tropical cyclone precipitation extremes over the US east coast. Proc. Natl. Acad. Sci. 118, e2105636118. https://doi.org/10.1073/pnas.2105636118.
McCarroll, D., Loader, N.J., 2004. Stable isotopes in tree rings. Quat. Sci. Rev. 23, 771–801. https://doi.org/10.1016/j.quascirev.2003.06.017. Isotopes in Quaternary Paleoenvironmental reconstruction.
Miller, D.L., Mora, C.I., Grissino-Mayer, H.D., Mock, C.J., Uhle, M.E., Sharp, Z., 2006. Tree-ring isotope records of tropical cyclone activity. Proc. Natl. Acad. Sci. 103, 14294–14297. https://doi.org/10.1073/pnas.0606549103.
Mitchell, T.J., Knapp, P.A., Ortegren, J.T., 2019. Tropical cyclone frequency inferred from intra- annual density fluctuations in longleaf pine in Florida, USA. Clim. Res. 78, 249–259. https://doi.org/10.3354/cr01573.
Moss, W.E., Crausbay, S.D., Rangwala, I., Wason, J.W., Trauernicht, C., Stevens-Rumann, C.S., Sala, A., Rottler, C.M., Pederson, G.T., Miller, B.W., Magness, D.R., Littell, J.S., Frelich, L.E., Frazier, A.G., Davis, K.T., Coop, J.D., Cartwright, J.M., Booth, R.K., 2024. Drought as an emergent driver of ecological transformation in the twenty-first century. BioScience 74, 524–538. https://doi.org/10.1093/biosci/biae050.
Nagavciuc, V., Ionita, M., Kern, Z., McCarroll, D., Popa, I., 2022. A ~700 years perspective on the 21st century drying in the eastern part of Europe based on δ18O in tree ring cellulose. Commun. Earth Environ. 3, 1–12. https://doi.org/10.1038/s43247-022-00605-4.
Nelson, W.L., 2008. Oxygen Isotope Ratios of Longleaf Pines as a Proxy of Past Hurricane Activity along the Atlantic Seaboard. Ph.D. Univ. of Tenn, Knoxville.
Neumann, C., 1987. The National Hurricane Center Risk Analysis Program (HURISK).
Nyarko, B.K., Kofi Essumang, D., Eghan, M.J., Reichert, B., Van De Giesen, N., Vlek, P., 2010. Use of isotopes to study floodplain wetland and river flow interaction in the White Volta River basin, Ghana. Isot. Environ. Health Stud. 46, 91–106. https://doi.org/10.1080/10256010903388543.
Oliva, F., Viau, A.E., Peros, M.C., Bouchard, M., 2018. Paleotempestology database for the western North Atlantic basin. The Holocene 28, 1664–1671. https://doi.org/10.1177/0959683618782598.
Paerl, H.W., Hall, N.S., Hounshell, A.G., Luettich, R.A., Rossignol, K.L., Osburn, C.L., Bales, J., 2019. Recent increase in catastrophic tropical cyclone flooding in coastal North Carolina, USA: long-term observations suggest a regime shift. Sci. Rep. 9, 10620. https://doi.org/10.1038/s41598-019-46928-9.
Pederson, N., Bell, A.R., Knight, T.A., Leland, C., Malcomb, N., Anchukaitis, K.J., Tackett, K., Scheff, J., Brice, A., Catron, B., Blozan, W., Riddle, J., 2012. A long-term perspective on a modern drought in the American southeast. Environ. Res. Lett. 7, 014034. https://doi.org/10.1088/1748-9326/7/1/014034.
Porter, T.J., Pisaric, M.F.J., Field, R.D., Kokelj, S.V., Edwards, T.W.D., deMontigny, P., Healy, R., LeGrande, A.N., 2014. Spring-summer temperatures since AD 1780 reconstructed from stable oxygen isotope ratios in white spruce tree-rings from the Mackenzie Delta, northwestern Canada. Clim. Dyn. 42, 771–785. https://doi.org/10.1007/s00382-013-1674-3.
R Core Team, 2024. R: A Language and Environment for Statistical Computing.
Raffalli-Delerce, G., Masson-Delmotte, V., Dupouey, J.L., Stievenard, M., Breda, N., Moisselin, J.M., 2004. Reconstruction of summer droughts using tree-ring cellulose isotopes: a calibration study with living oaks from Brittany (western France), 56, 160–174. https://doi.org/10.3402/tellusb.v56i2.16405.
Ramesh, R., Bhattacharya, S.K., Gopalan, K., 1986. Climatic correlations in the stable isotope records of silver fir (Abies pindrow) trees from Kashmir, India. Earth Planet. Sci. Lett. 79, 66–74. https://doi.org/10.1016/0012-821X(86)90041-5.
Roden, J.S., Ehleringer, J.R., 2000. Hydrogen and oxygen isotope ratios of tree ring cellulose for Field-grown riparian trees. Oecologia 123, 481–489.
Rodriguez-Caton, M., Morales, M.S., Rao, M.P., Nixon, T., Vuille, M., Rivera, J.A., Oelkers, R., Christie, D.A., Varuolo-Clarke, A.M., Ferrero, M.E., Magney, T., Daux, V., Villalba, R., Andreu-Hayles, L., 2024. A 300-year tree-ring δ18O-based precipitation reconstruction for the south American Altiplano highlights decadal hydroclimate teleconnections. Commun. Earth Environ. 5, 1–13. https://doi.org/10.1038/s43247-024-01385-9.
Roth, D., Accessed 2023. Tropical cyclone rainfall data [WWW document]. URL. https://www.wpc.ncep.noaa.gov/tropical/rain/tcrainfall.html.
Sadeghi, S., Tootle, G., Elliott, E., Lakshmi, V., Therrell, M., Kalra, A., 2019a. Implications of the 2015–2016 El Niño on coastal Mississippi-Alabama streamflow and agriculture. Hydrology 6, 96. https://doi.org/10.3390/hydrology6040096.
Sadeghi, S., Tootle, G., Elliott, E., Lakshmi, V., Therrell, M., Kam, J., Bearden, B., 2019b. Atlantic Ocean Sea surface temperatures and Southeast United States streamflow variability: associations with the recent multi-decadal decline. J. Hydrol. 576, 422–429. https://doi.org/10.1016/j.jhydrol.2019.06.051.
Scheidegger, Y., Saurer, M., Bahn, M., Siegwolf, R., 2000. Linking stable oxygen and carbon isotopes with stomatal conductance and photosynthetic capacity: a conceptual model. Oecologia 125, 350–357. https://doi.org/10.1007/s004420000466.
Schweingruber, F.H., 1993. Trees and Wood in Dendrochronology: Morphological, Anatomical, and Tree-Ring Analytical Characteristics of Trees Frequently Used in Dendrochronology. Springer Science & Business Media.
Sheppard, P.R., Ort, M.H., Anderson, K.C., Elson, M.D., Vázquez-selem, L., Clemens, A. W., Little, N.C., Speakman, R.J., 2008. Multiple dendrochronological signals indicate the eruption of ParíCutin volcano, Michoacán, Mexico. Tree-Ring Res. 64, 97–108. https://doi.org/10.3959/2008-3.1.
Song, X., Clark, K.S., Helliker, B.R., 2014. Interpreting species-specific variation in tree-ring oxygen isotope ratios among three temperate forest trees. Plant Cell Environ. 37, 2169–2182. https://doi.org/10.1111/pce.12317.
Stahle, D.W., Cleaveland, M.K., 1992. Reconstruction and analysis of spring rainfall over the southeastern U.S. for the past 1000 years. Bull. Am. Meteorol. Soc. 73, 1947–1961.
Stahle, D.W., Cleaveland, M.K., 1994. Tree-ring reconstructed rainfall over the Southeastern U.S.A. during the medieval warm period and little ice age. In: Hughes, M.K., Diaz, H.F. (Eds.), The Medieval Warm Period. Springer Netherlands, Dordrecht, pp. 199–212. https://doi.org/10.1007/978-94-011-1186-7_5.
Stahle, D.W., Cleaveland, M.K., Hehr, J.G., 1985a. A 450-year drought reconstruction for Arkansas, United States. Nature 316, 530–532. https://doi.org/10.1038/316530a0.
Stahle, David W., Cook, E.R., White, J.W.C., 1985b. Tree-ring dating of baldcypress and the potential for millennia-long chronologies in the southeast. Am. Antiq. 50, 796–802. https://doi.org/10.2307/280168.
Stahle, D.W., Cleaveland, M.K., Blanton, D.B., Therrell, M.D., Gay, D.A., 1998. The lost colony and jamestown droughts. Science 280, 564–567. https://doi.org/10.1126/science.280.5363.564.
Stahle, D.W., Fye, F.K., Therrell, M.D., 2003. Interannual to decadal climate and streamflow variability estimated from tree rings. In: developments in quaternary sciences, the quaternary period in the United States. Elsevier, pp. 491–504. https://doi.org/10.1016/S1571-0866(03)01023-6.
Stahle, D.W., Burnette, D.J., Villanueva, J., Cerano, J., Fye, F.K., Griffin, R.D., Cleaveland, M.K., Stahle, D.K., Edmondson, J.R., Wolff, K.P., 2012. Tree-ring analysis of ancient baldcypress trees and subfossil wood. Quat. Sci. Rev. 34, 1–15. https://doi.org/10.1016/j.quascirev.2011.11.005.
Sternberg, L., Deniro, M.J., 1983. Isotopic composition of cellulose from C3, C4, and CAM plants growing near one another. Science 220, 947–949. https://doi.org/10.1126/science.220.4600.947.
Szejner, P., Belmecheri, S., Babst, F., Wright, W.E., Frank, D.C., Hu, J., Monson, R.K., 2021. Stable isotopes of tree rings reveal seasonal-to-decadal patterns during the emergence of a megadrought in the southwestern US. Oecologia 197, 1079–1094.
Tang, K., Feng, X., 2001. The effect of soil hydrology on the oxygen and hydrogen isotopic compositions of plants' source water. Earth Planet. Sci. Lett. 185, 355–367. https://doi.org/10.1016/S0012-821X(00)00385-X.
Therrell, M.D., Bialecki, M.B., 2015. A multi-century tree-ring record of spring flooding on the Mississippi River. J. Hydrol. Adv. Paleohydrol. Res. Applic. 529, 490–498. https://doi.org/10.1016/j.jhydrol.2014.11.005.
Therrell, M.D., Elliott, E.A., Meko, M.D., Bregy, J.C., Tucker, C.S., Harley, G.L., Maxwell, J.T., Tootle, G.A., 2020. Streamflow variability indicated by false rings in bald cypress (Taxodium distichum (L.) rich.). Forests 11, 1100. https://doi.org/10.3390/f11101100.
Treydte, K., Frank, D., Esper, J., Andreu, L., Bednarz, Z., Berninger, F., Boettger, T., D'Alessandro, C.M., Etien, N., Filot, M., Grabner, M., Guillemin, M.T., Gutierrez, E., Haupt, M., Helle, G., Hilasvuori, E., Jungner, H., Kalela-Brundin, M., Krapiec, M., Leuenberger, M., Loader, N.J., Masson-Delmotte, V., Pazdur, A., Pawelczyk, S., Pierre, M., Planells, O., Pukiene, R., Reynolds-Henne, C.E., Rinne, K.T., Saracino, A., Saurer, M., Sonninen, E., Stievenard, M., Switsur, V.R., Szczepanek, M., Szychowska-Krapiec, E., Todaro, L., Waterhouse, J.S., Weigl, M., Schleser, G.H., 2007. Signal strength and climate calibration of a European tree-ring isotope network. Geophys. Res. Lett. 34. https://doi.org/10.1029/2007GL031106.
Trouet, V., Oldenborgh, G.J.V., 2013. KNMI climate explorer: a web-based research tool for high-resolution paleoclimatology. trre 69, 3–13. https://doi.org/10.3959/1536-1098-69.1.3.
Tucker, C.S., Trepanier, J.C., Harley, G.L., DeLong, K.L., 2018. Recording Tropical Cyclone Activity from 1909 to 2014 along the Northern Gulf of Mexico using Maritime Slash Pine Trees (Pinus elliottii var. elliottii Engelm.).
Tucker, C.S., Pearl, J.K., Elliott, E.A., Bregy, J.C., Friedman, J.M., Therrell, M.D., 2022. Baldcypress false ring formation linked to summer hydroclimatic extremes in the southeastern United States. Environ. Res. Lett. 17, 114030. https://doi.org/10.1088/1748-9326/ac9745.
U.S. Geological Survey, 2023. USGS 02361000 choctawhatchee river near Newton, AL. http://dx.doi.org/10.5066/F7P55KJNUR.

Vines, M., Tootle, G., Terry, L., Elliott, E., Corbin, J., Harley, G.L., Kam, J., Sadeghi, S., Therrell, M., 2021. A paleo perspective of Alabama and Florida (USA) interstate streamflow. Water 13, 657. https://doi.org/10.3390/w13050657.

Wallace, E.J., Donnelly, J.P., van Hengstum, P.J., Wiman, C., Sullivan, R.M., Winkler, T. S., d'Entremont, N.E., Toomey, M., Albury, N., 2019. Intense hurricane activity over the past 1500 years at South Andros Island, the Bahamas. Paleoceanography and Paleoclimatology 34, 1761–1783. https://doi.org/10.1029/2019PA003665.

Weigl, M., Grabner, M., Helle, G., Schleser, G.H., Wimmer, R., 2008. Characteristics of radial growth and stable isotopes in a single oak tree to be used in climate studies. Sci. Total Environ. 393, 154–161. https://doi.org/10.1016/j.scitotenv.2007.12.016.

Williams, A.P., Allen, C.D., Macalady, A.K., Griffin, D., Woodhouse, C.A., Meko, D.M., Swetnam, T.W., Rauscher, S.A., Seager, R., Grissino-Mayer, H.D., Dean, J.S., Cook, E. R., Gangodagamage, C., Cai, M., McDowell, N.G., 2013. Temperature as a potent driver of regional forest drought stress and tree mortality. Nat. Clim. Chang. 3, 292–297. https://doi.org/10.1038/nclimate1693.

Williams, A.P., Cook, E.R., Smerdon, J.E., Cook, B.I., Abatzoglou, J.T., Bolles, K., Baek, S. H., Badger, A.M., Livneh, B., 2020. Large contribution from anthropogenic warming to an emerging North American megadrought. Science 368, 314–318. https://doi.org/10.1126/science.aaz9600.

Williams, A.P., Cook, B.I., Smerdon, J.E., 2022. Rapid intensification of the emerging southwestern North American megadrought in 2020–2021. Nat. Clim. Chang. 12, 232–234. https://doi.org/10.1038/s41558-022-01290-z.

Winter, T.C., Harvey, J.W., Franke, O.L., Alley, W.M., 1998. Ground Water and Surface Water: A Single Resource (No. 1139), Circular. U.S. Geological Survey. https://doi.org/10.3133/cir1139.

Woodhouse, C.A., Gray, S.T., Meko, D.M., 2006. Updated streamflow reconstructions for the upper Colorado River basin. Water Resour. Res. 42. https://doi.org/10.1029/2005WR004455.

Woodhouse, C.A., Meko, D.M., MacDonald, G.M., Stahle, D.W., Cook, E.R., 2010. A 1,200-year perspective of 21st century drought in southwestern North America. Proc. Natl. Acad. Sci. USA 107, 21283–21288. https://doi.org/10.1073/pnas.0911197107.

Xu, C., Zhao, Q., An, W., Wang, S., Tan, N., Sano, M., Nakatsuka, T., Borhara, K., Guo, Z., 2021. Tree-ring oxygen isotope across monsoon Asia: common signal and local influence. Quat. Sci. Rev. 269, 107156.

Young, G.H.F., Demmler, J.C., Gunnarson, B.E., Kirchhefer, A.J., Loader, N.J., McCarroll, D., 2011. Age trends in tree ring growth and isotopic archives: a case study of Pinus sylvestris L. from northwestern Norway. Glob. Biogeochem. Cycles 25. https://doi.org/10.1029/2010GB003913.

Zang, C., Biondi, F., 2015. Treeclim: an R package for the numerical calibration of proxy-climate relationships. Ecography 38, 431–436. https://doi.org/10.1111/ecog.01335.

Zimmermann, U., Ehhalt, D., Muennich, K.O., 1967. Soil-Water Movement and Evapotranspiration: Changes in the Isotopic Composition of the Water. IAEA, International Atomic Energy Agency (IAEA).